SS activity assay

Liver microsomal protein was obtained as described above, and stored in aliquots at −80°C. SS activities were measured according to a modified method of Cohen et al. (18, 24). In brief, the microsome fractions (~20 μg) were incubated in 50 μl of a buffer containing 20 μM [1-^{3}H]farnesyl pyrophosphate (25 μCi/μmol; NEN Life Science Products, Inc.), 1 mM NADPH, 5 mM $MgCl_2$, 6 mM glutathione, and 100 mM potassium phosphate, pH 7.4, at 37°C for 15 min. The reaction was terminated by the addition of 150 μl chloroform-methanol (1:2; v/v) containing 0.2% unlabeled squalene. After 50 μl of chloroform and 50 μl of 3 M NaOH were added, the reaction mixtures were vortexed and centrifuged. The infranatant organic phase was used for the determination of the radioactivities in the squalene produced.

Plasma lipids and lipoprotein analyses

Plasma levels of total cholesterol (TC), triglycerides (TGs), and FFAs were determined enzymatically using kits: Determiner TC555 (Kyowa Medex), Triglyceride-G, and NEFA-C (WAKO Pure Chemicals). Lipoproteins were fractionated by HPLC as described (25), and the cholesterol contents in each lipoprotein fraction were determined.

Histology

Tissues were fixed with neutral-buffered formalin, embedded in paraffin, and stained with hematoxylin and eosin. Ki-67 staining was performed using rat ant-mouse Ki-67 antibody (DAKO; Glostrup, Denmark). Apoptosis was detected by terminal deoxyribonucleotidyl transferase-mediated dUTP nick end labeling (TUNEL) staining using the in situ Apoptosis Detection Kit (TaKaRa, Japan) according to the instruction manual. The number of cells positive for staining with Ki-67 or TUNEL was counted in each field of representative slides from three independent experiments at a magnification of ×100.

Tissue and cellular lipids

Lipids were extracted from tissues by the method of Folch, Lees, and Sloane Stanley (26). TC was determined by fluorometric microassay according to a modified method of Heider and Boyett (27) with the exception that 0.01% (v/v) Triton X-100 was used instead of Carbowax-600. TG was determined enzymatically using a kit (Triglyceride-G, WAKO Pure Chemicals).

HMG-CoA reductase activity assay

Liver microsomal proteins were prepared as described above. HMG-CoA reductase activities were measured essentially as described previously (9). Briefly, the microsome fractions (50 μg) were incubated in 20 μl of a buffer containing 110 μM DL-[3-^{14}C]HMG-CoA (4.5 μCi/μmol; NEN Life Science Products, Inc.), 5 mM NADPH, 10 mM EDTA, 10 mM dithiothreitol, and 100 mM potassium phosphate, pH 7.4, at 37°C for 30 min. The reaction was terminated by the addition of 10 μl of 2 N HCl and incubated for another 30 min at 37°C to lactonize the mevalonate formed. The [^{14}C]mevalonate was isolated by TLC and counted using [^{3}H]mevalonate as an internal standard. HMG-CoA reductase activity is expressed as picomoles of [^{14}C]mevalonate formed per minute per mg of protein.

Measurement of hepatic cholesterol synthesis in vivo

Seven days after administration of adenovirus to mice, cholesterol synthesis in the liver was estimated during the mid light cycle as previously described (18, 19, 28). In brief, animals were given food and water ad libitum and injected intraperitoneally with 37 kBq/kg body weight of [2-^{14}C]acetate (NEN Life Science Products, Inc.). After 1 h, animals were euthanized and the liver was removed. Two portions of the liver (200–300 mg/each) were saponified, and the digitonin-precipitable sterols were isolated for the measurement of radioactivities. The results were expressed as ^{14}C dpm/100 mg of wet weight of liver/h.

Measurement of cellular cholesterol synthesis in vitro

Cholesterol biosynthesis in vitro was determined essentially as described previously (29, 30). Briefly, McARH7777 cells (American Type Culture Collection) were grown in DMEM containing 10% FBS and 10% fetal horse serum and were plated on day 0 at a density of 2.5×10^{4} cells per square centimeter into 24-well collagen-coated plates (IWAKI). On day 1, transfection of recombinant adenovirus (Ad-LacZ or Ad-SS) was performed at the indicated m.o.i. On day 3, [2-^{14}C]acetate (51 mCi/mmol; NEN Life Science Products, Inc.) was added to a final concentration of 10 μCi per well. After incubation for 5 h, the medium was removed and centrifuged. The cells were harvested by scraping into 100 μl of 0.1 N sodium hydroxide, followed by 100 μl of water. Radiolabeled lipids were saponified by 15% KOH, extracted by petroleum ether. The content of ^{14}C-labeled squalene, ^{14}C-labeled cholesterol, and ^{14}C-labeled fatty acids in the cells and in the medium was quantified by TLC and scintillation counting. The cellular protein was measured by the BCA Protein Assay Kit (Pierce Chemical Co., Rockford, IL).

Assay of microsomal ACAT activity

Liver was homogenized in buffer A (0.25 M sucrose, 1 mM EDTA, 2 μg/ml leupeptin, and 50 mM Tris-HCl, pH 7.0) and centrifuged at 100,000 *g* for 45 min at 4°C. The pellets were resuspended and used for the assay. ACAT activity in microsomes was determined by the rate of incorporation of [1-^{14}C]oleoyl-CoA (53.5 mCi/mmol; NEN Life Science Products, Inc.) into the cholesteryl ester fraction according to Yagyu et al. (25).

VLDL secretion rate

Secretion rates of TG or cholesterol in vivo were estimated by the intravenous administration of Triton WR1339 as described previously (31). Plasma levels of TG or cholesterol were measured at 1, 2, 3, and 4 h after the treatment. Aliquots of plasma were subjected to sequential ultracentrifugation to separate lipoprotein fractions using S100AT3 angle rotor for himac CS120GXL (HITACHI). In brief, 60 μl of plasma was mixed with 60 μl of saline and centrifuged at 188,000 *g* for 3 h at 16°C. Sixty microliters was aspirated from the bottom by Hamilton syringe and mixed with a KBr solution (d = 1.12) and centrifuged at 188,000 *g* for 5 h at 16°C. The remaining top fraction was used as the VLDL fraction. Sixty microliters was aspirated as described above and used as the HDL fraction, and the remaining top fraction was used as the IDL/LDL fraction.

Statistical analyses

All values are given as mean ± SE, and differences between groups were evaluated with Student's *t*-test or ANOVA, unless otherwise stated. All calculations were performed with STAT view, version 5.0, for Macintosh (SAS Institute).

RESULTS

Intravenous injection of Ad-SS elicited an 11-fold increase in mRNA expression of mouse SS in the liver as

TABLE 1. Relative amounts of mRNAs in the livers

Gene	PBS	Ad-LacZ	Ad-SS
HMG-CoA reductase	1.00 ± 0.14	1.19 ± 0.08	0.72 ± 0.13[b]
Squalene synthase	1.00 ± 0.40	1.24 ± 0.21	13.43 ± 2.20[b]
Squalene epoxydase	1.00 ± 0.18	1.26 ± 0.28[a]	0.35 ± 0.03[b]
Lanosterol 14α-demethylase	1.00 ± 0.23	1.34 ± 0.23	0.41 ± 0.07[b]
SREBP-1a	1.00 ± 0.09	0.91 ± 0.08[a]	0.54 ± 0.06[b]
Fatty acid synthase	1.00 ± 0.07	0.53 ± 0.06[a]	0.46 ± 0.04
ACAT2	1.00 ± 0.10	1.61 ± 0.24[a]	0.49 ± 0.04[b]
ApoB	1.00 ± 0.17	1.08 ± 0.06	0.55 ± 0.05[b]
LDLR	1.00 ± 0.05	0.90 ± 0.04	0.47 ± 0.04[b]
CYP7A	1.00 ± 0.37	6.75 ± 2.01[a]	3.40 ± 0.49
ABCA1	1.00 ± 0.08	0.79 ± 0.03[a]	0.52 ± 0.03[b]

Seven days after intravenous injection of adenovirus into C57BL/6 mice (n = 4), total RNA was isolated from the livers and used for real-time PCR analysis. Values are indicated as means ± SE. HMG-CoA reductase, 3-hydroxy-3-methyglutaryl-CoA reductase; SREBP, sterol-regulatory element binding protein; ACAT, acyl-CoA:cholesterol acyltransferase; apoB, apolipoprotein B; LDLR, LDL receptor; CYP7A, cholesterol 7α-hydroxylase; ABCA1, ATP binding cassette transporter A1.

[a] $P < 0.05$ vs. PBS by ANOVA and Fisher's protected least significant difference (PLSD) test.

[b] $P < 0.05$ vs. Ad-LacZ by ANOVA and Fisher's PLSD.

compared with Ad-LacZ (**Table 1**). In parallel, mouse SS protein was markedly expressed in liver of Ad-SS-injected mice (**Fig. 1A**). Hepatic SS activities were also remarkably increased in the liver, by 52-fold (Fig. 1B).

To determine whether the overexpressed SS accompanied increased cholesterol synthesis, we measured the amounts of cholesterol synthesized from acetyl-CoA in the liver (**Fig. 2A**). Although the use of acetic acid as a substrate for cholesterol biosynthesis poses several limitations to the interpretation of the results (32), we presume that overexpression of SS is unlikely to affect other potential confounding factors such as transmembrane permeability of acetic acid and/or differential dilution by the intracellular pool of acetyl-CoA. Hepatic cholesterol synthesis was increased 2-fold. Given that HMG-CoA reductase is the

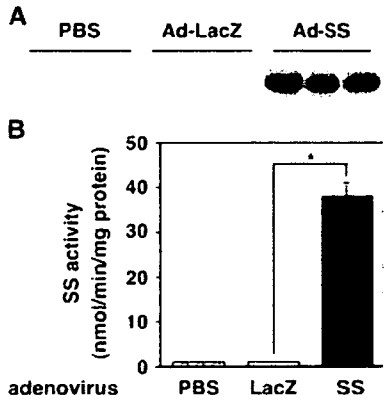

Fig. 1. Expression of squalene synthase (SS). Seven days after intravenous injection of adenovirus into C57BL/6 mice (n = 6), livers were excised and used for Western blot analysis of SS (A) and for measurements of SS activities (B). *, $P < 0.0001$ vs. Ad-LacZ. Three representative samples were used for Western blot analysis. Error bars represent standard deviation.

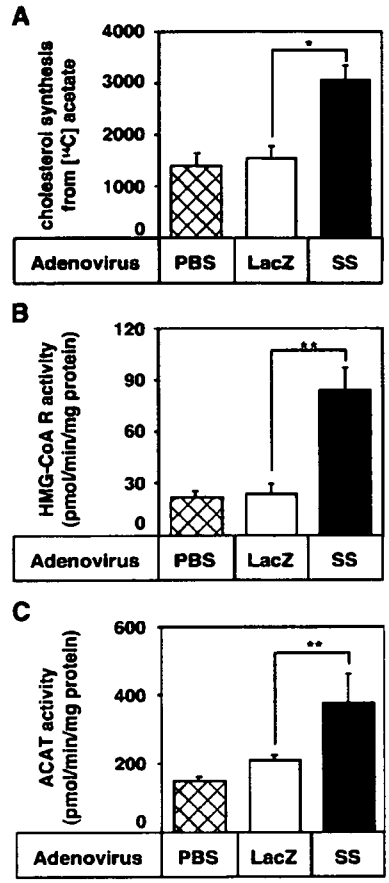

Fig. 2. Cholesterol synthesis, HMG-CoA reductase, and ACAT activities in the liver. Seven days after intravenous injection of adenovirus into C57BL/6 mice (n = 6), rates of hepatic cholesterol synthesis (A) and HMG-CoA reductase (B) and ACAT activities (C) in the livers were measured. *, $P < 0.05$ and **, $P < 0.0001$ vs. Ad-LacZ. Error bars represent standard deviation.

rate-limiting enzyme of cholesterol synthesis, we measured the activities of HMG-CoA reductase in the microsome fraction of the liver (Fig. 2B). There was a 3.6-fold increase in the HMG-CoA reductase activities in the Ad-SS-injected mice compared with Ad-LacZ-injected mice. To determine whether the increase in the HMG-CoA reductase activities was associated with induction of the mRNA expression, we performed RT-PCR of HMG-CoA reductase along with other enzymes in the cholesterol synthetic pathway (Table 1). The hepatic mRNA level of HMG-CoA reductase was rather decreased, by 39%, in the Ad-SS-treated mice, indicating that the increased enzymatic activity was at posttranscriptional level. More notably, the relative mRNA expression of enzymes catalyzing the steps downstream of HMG-CoA reductase, such as squalene epoxidase and lanosterol 14α-demethylase, was significantly suppressed in the Ad-SS-injected mice by 72% and 69%, respectively. To estimate the protein expression of HMG-CoA reductase in the liver membrane fraction, we performed Western blot analysis. Although we tried to

detect HMG-CoA reductase protein expression by using two different antibodies, we failed to detect a 97 kDa band that reportedly corresponds to HMG-CoA reductase (data not shown).

To determine whether the increased cholesterol synthesis in the liver overexpressing SS affected hepatic cholesterol contents, we measured lipid contents in the liver (**Table 2**). The weight of the liver was increased by 37% in Ad-SS-injected mice compared with Ad-LacZ-injected mice. Cholesterol contents per weight of wet tissue were not different between the Ad-LacZ- and Ad-SS-injected mice, whereas TG contents per weight of wet tissue were decreased by 35% in Ad-SS-injected mice. Thus, cholesterol content in the whole liver was increased in proportion to the increase in liver weight. To determine the reasons for the hepatomegaly in Ad-SS-injected mice, we performed histology (**Fig. 3**). Hematoxylin and eosin staining showed negligible infiltration of inflammatory cells; there were no differences between the Ad-LacZ- and Ad-SS-injected mice. The number of Ki-67-positive cells, which are correlated with cell proliferation activity (33), was significantly increased in the livers of Ad-SS-injected mice compared with Ad-LacZ-injected mice (17.7 ± 2.3 vs. 0 ± 0 cells/field; $P < 0.01$), whereas the number of TUNEL-positive cells was not different between the Ad-LacZ- and Ad-SS-injected mice. These results indicate that overexpression of SS stimulates cell proliferation of hepatocytes, thereby leading to hepatomegaly.

Plasma lipoprotein profiles were determined 7 days after the injection of the virus into wild-type mice (**Fig. 4A** and **Table 3**). Plasma cholesterol levels were significantly increased, by 66%, in Ad-SS-injected mice compared with Ad-LacZ-injected mice, whereas there were no significant differences in plasma levels of either TG or FFA. HPLC lipoprotein analyses revealed that LDL- and HDL-cholesterol levels were increased by 1.9- and 1.3-fold, respectively.

To determine how the hepatic overexpression of SS led to hypercholesterolemia, we determined hepatic VLDL secretion rates (**Fig. 5**). Rates of increases in plasma cholesterol levels after the injection of Triton WR1339 were significantly increased in Ad-SS-injected mice compared with Ad-LacZ-injected mice (Fig. 5B), whereas those in plasma TG levels were not different between the two groups (Fig. 5A). These results indicate that the increase in plasma LDL-cholesterol levels resulted primarily from the secretion of cholesterol-rich VLDL from the liver. Indeed, the

TABLE 2. Lipid contents of the livers

	Ad-LacZ	Ad-SS
Body weight (g)	24.1 ± 0.8	25.1 ± 0.6
Liver weight (g)	1.465 ± 0.61	2.003 ± 0.059[a]
TC (mg/g wet tissue)	1.101 ± 0.038	1.310 ± 0.132
TG (mg/g wet tissue)	3.672 ± 0.228	2.387 ± 0.310

Seven days after intravenous injection of adenovirus into C57BL/6 mice (n = 6), lipids were extracted from the livers by the method of Folch, Lees, and Sloane Stanley (26). TC and TG were measured enzymaticaly. TC, total cholesterol; TG, triglyceride. Values are indicated as means ± SD.

[a] $P < 0.0001$ vs. Ad-LacZ.

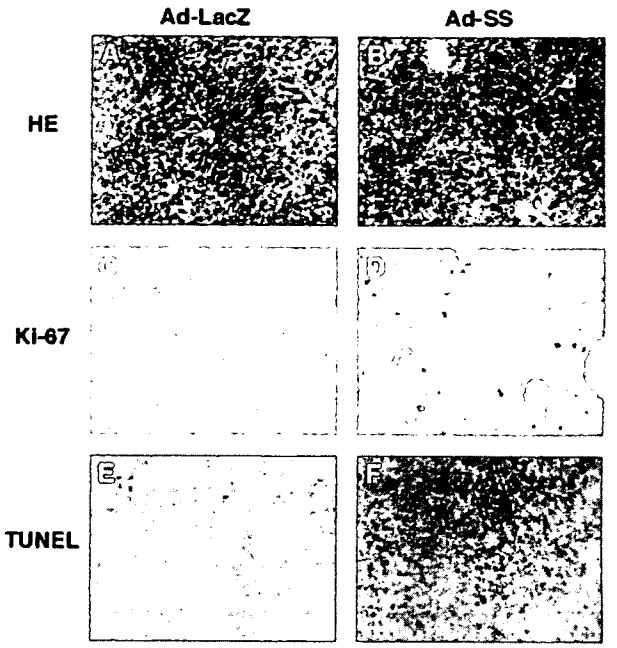

Fig. 3. Histology of the liver. Seven days after intravenous injection of adenovirus into C57BL/6 mice, liver samples from mice overexpressing Ad-LacZ (A, C, E) or Ad-SS (B, D, F) were fixed in neutral-buffered formalin and embedded in paraffin. A, B: Tissue sections were stained with hematoxylin and eosin (HE). C, D: Ki-67 staining was performed using rat anti-mouse Ki-67 antibody. Ki-positive cells are brown. E, F: Apoptosis was detected by terminal deoxyribonucleotidyl transferase-mediated dUTP nick end labeling (TUNEL) staining using the in situ Apoptosis Detection Kit. TUNEL-positive cells are brown.

cholesterol/protein ratio of VLDL from Ad-SS-injected mice was 1.6-fold higher than that of VLDL from Ad-LacZ-injected mice at 4 h after the injection of Triton WR1339 (**Table 4**). Cholesterol in the IDL/LDL fraction did not increase at 4 h after the injection of Triton WR1339 (Ad-LacZ, from 10.5 ± 0.8 mg/dl to 9.8 ± 0.7 mg/dl; Ad-SS, from 30.3 ± 3.6 mg/dl to 28.4 ± 2.7 mg/dl). Thus, the contribution of increased secretion of LDL to the development of hypercholesterolemia was negligible. Consistent with the production of cholesterol-rich VLDL, ACAT activities in the liver microsome were significantly increased, by 81% (Fig. 2C). However, mRNA expression levels of ACAT-2 or apoB in Ad-SS-injected mice were rather suppressed (Table 1).

It is conceivable that increased cholesterol synthesis suppresses the expression of LDLR, the major pathway for LDL removal, and thereby delays the plasma clearance of LDL. To explore this possibility, we measured relative mRNA expression of LDLR in the liver. It was decreased by 48% in the Ad-SS-injected mice compared with the Ad-LacZ-injected mice (Table 1).

Cholesterol could be eliminated from the liver as bile acids. The mRNA level of cholesterol 7α-hydroxylase, the rate-limiting enzyme for bile acid synthesis, however, was not increased (Fig. 1). Cholesterol could be secreted into

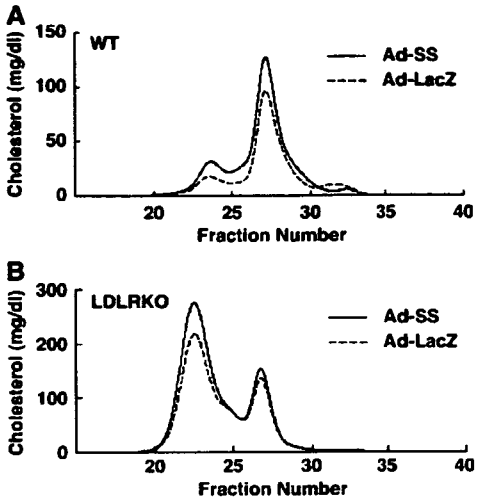

Fig. 4. Plasma lipoprotein profiles. Seven days after intravenous injection of adenovirus into C57BL/6 mice (A) (n = 6) or LDL receptor (LDLR) knockout mice (B) (n = 6), blood was collected after a 4 h fast. Pooled plasma was subjected to HPLC lipoprotein analyses. WT, wild type; LDLRKO, LDLR knockout.

circulation directly from the liver via ABCA1, for example. However, mRNA expression of ABCA1 was decreased by 34% (Table 1).

Secretion of cholesterol-rich VLDL as a major cause of hypercholesterolemia was confirmed by an experiment in which Ad-SS was injected into LDLR knockout mice. In the absence of LDLR, plasma cholesterol levels are determined primarily by the VLDL production rate, because the difference in the LDL clearance is negligible. TC levels were increased by 1.3-fold (Table 3). HPLC lipoprotein analyses revealed that cholesterol was increased mainly in the non-HDL fraction (Fig. 4B, Table 3).

To further verify the notion that the overexpression of SS is associated with increased cholesterol synthesis and

TABLE 3. Changes in plasma lipids and lipoproteins in wild-type or LDLR knockout mice

Mice	Lipids and Lipoproteins	Ad-LacZ	Ad-SS
Wild-type	TC (mg/dl)	83.1 ± 3.9	137.6 ± 4.4[a]
	TG (mg/dl)	50.7 ± 1.9	44.2 ± 2.3
	FFA (μM)	684.2 ± 101.5	583.8 ± 56.4
	VLDL (mg/dl)	3.50 ± 0.39	4.77 ± 0.40
	LDL (mg/dl)	15.68 ± 1.61	29.58 ± 3.62[a]
	HDL (mg/dl)	63.25 ± 2.81	84.07 ± 0.83[a]
LDLRKO	TC (mg/dl)	260.5 ± 9.6	334.7 ± 22.3[a]
	TG (mg/dl)	111.3 ± 6.6	117.8 ± 6.2
	FFA (μM)	421.6 ± 20.0	383.0 ± 23.9
	VLDL (mg/dl)	53.4	71.6
	LDL (mg/dl)	184.5	213.3
	HDL (mg/dl)	93.8	104.0

Seven days after intravenous injection of adenovirus into wild-type C57BL/6 mice (n = 6) or LDL receptor knockout (LDLRKO) mice (n = 6), blood was collected after a 4 h fast. Plasma was subjected to HPLC lipoprotein analyses individually. Pooled plasma was used to obtain lipoprotein data for LDLRKO mice. Values are indicated as means ± SD.

[a] $P < 0.05$ vs. Ad-LacZ.

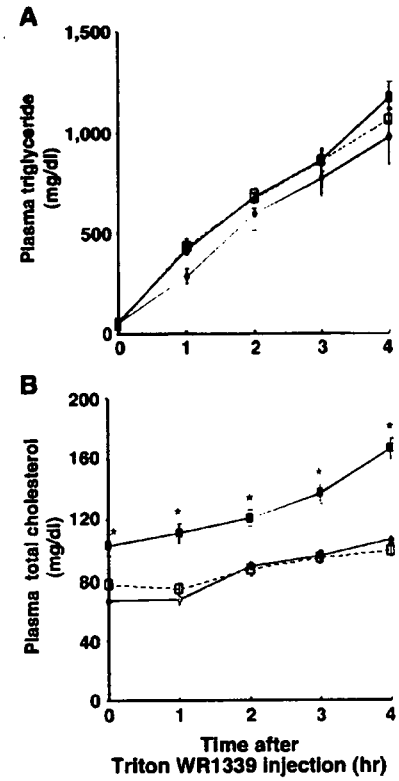

Fig. 5. Hepatic VLDL secretion. Seven days after intravenous injection of PBS (n = 4), Ad-LacZ (n = 6), or Ad-SS (n = 6) into C57BL/6 mice, VLDL secretion rates were determined by the increments of plasma levels of triglyceride (A) or cholesterol (B) after the intravenous injection of Triton WR1339. VLDL-cholesterol secretion rate in Ad-SS-injected mice was larger than that in Ad-LacZ-injected mice. *, $P < 0.05$ vs. Ad-LacZ by 2-way ANOVA and Fisher's protected least significant difference test. Dotted lines with open squares denote Ad-LacZ; solid lines with closed diamonds denote PBS; solid lines with closed squares denote Ad-SS.

VLDL secretion, we performed in vitro experiments using McARH7777 cells (**Fig. 6**). Cultured McARH7777 cells were infected with either Ad-LacZ or Ad-SS. After 48 h, [^{14}C]acetate was added to the culture, and the cells were incubated for 5 h. Radiolabeled lipids were extracted from the cells and medium, and the radioactivities incorporated into the sterols and fatty acids (unesterified plus esterified) were determined after they were resolved by TLC. As expected, Ad-SS-infected cells synthesized larger amounts of cholesterol than did the control cells infected with Ad-LacZ. Synthesis of fatty acids was also increased. Furthermore, secretion of cholesterol and fatty acids into the culture medium was also stimulated in Ad-SS-infected cells more than in Ad-LacZ-infected cells.

DISCUSSION

In the present study, we showed that overexpression of SS in the liver causes increased cholesterol biosynthesis

TABLE 4. Lipid contents in VLDL and IDL/LDL before and after intravenous injection of Triton WR1339

Lipid	h	PBS	Ad-LacZ	Ad-SS
			μg/mg protein	
Triglyceride				
VLDL	0	33.7 ± 2.5	31.2 ± 4.7	30.7 ± 1.8
	4	2,755 ± 559	2,311 ± 101	2,457 ± 167
IDL/LDL	0	27.2 ± 2.6	38.3 ± 7.7	38.3 ± 3.7
	4	79.9 ± 11.8	78.1 ± 12.8	110 ± 17
Cholesterol				
VLDL	0	26.2 ± 1.6	23.0 ± 1.7	30.3 ± 1.9[a]
	4	225 ± 29	176 ± 10	277 ± 17[a]
IDL/LDL	0	40.7 ± 6.3	32.9 ± 4.5	77.5 ± 7.9[a]
	4	81.4 ± 9.5	48.6 ± 5.7	156 ± 17[a]

Seven days after intravenous injection of PBS (n = 4), Ad-LacZ (n = 6), or Ad-SS (n = 6) into wild-type C57BL/6 mice, Triton WR1339 was injected intravenously. Blood was collected before and 4 h after the injection. Plasma was subjected to sequential analytical ultracentrifugation. Concentrations of protein, TG, and cholesterol were determined. Values are indicated as means ± SE.

[a] $P < 0.05$ vs. Ad-LacZ by ANOVA and Fisher's PLSD.

and hypercholesterolemia, which is the first in vivo evidence that SS plays a regulatory role in cholesterol metabolism, and is a mirror image of previous observations by others that SS inhibitors possess cholesterol-lowering activity primarily through inhibition of hepatic VLDL production (16, 17, 34). Other new findings in the current paper are as follows: *1*) HMG-CoA reductase activity is upregulated in spite of downregulation of its own mRNA expression. *2*) Secretion of cholesterol-rich VLDL and possibly downregulation of LDLR are responsible for the development of hypercholesterolemia. *3*) Increased cholesterol synthesis is associated with hepatomegaly due to increased proliferation of hepatocytes. *4*) Genes of enzymes in the cholesterol synthetic pathway, including the enzymes downstream of SS, such as squalene epoxidase and lanosterol 14α-demethylase, are downregulated.

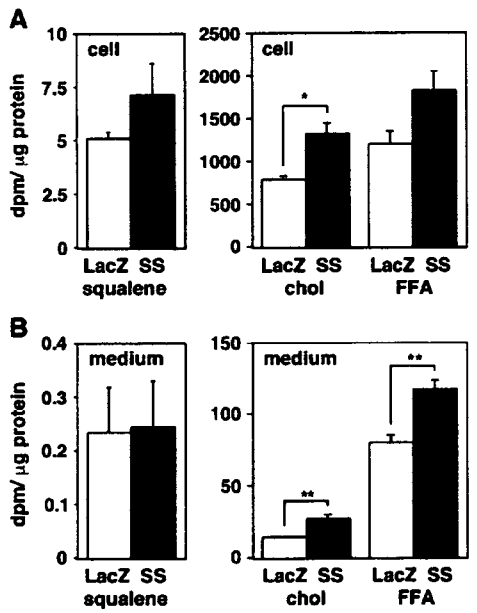

Fig. 6. Lipid synthesis and secretion in McARH7777 cells. McARH7777 cells were transfected with recombinant adenovirus [Ad-LacZ (open bars) and Ad-SS (closed bars)], and after 48 h, [^{14}C]acetate was added to a final concentration of 28.6 μCi/ml. After 5 h of incubation, the media (B) were removed and the cells (A) were harvested. Radiolabeled sterols and fatty acids were extracted and resolved by TLC, and the content of ^{14}C-labeled sterol and fatty acids in cells and media were measured. *, $P < 0.05$ and **, $P < 0.01$ vs. Ad-LacZ. Chol, cholesterol. Error bars represent standard deviation.

The mRNA expression of enzymes in the cholesterol biosynthetic pathway, such as HMG-CoA reductase, squalene epoxidase, and lanosterol 14α-demethylase, was downregulated (Table 1). The downregulation of these genes might be mediated through a negative feedback regulation by the end product, cholesterol, which was overproduced by the liver (Fig. 2). The downregulation of the genes for squalene epoxidase and lanosterol 14α-demethylase suggests that there are no other rate-limiting steps in the cholesterol biosynthetic pathway past SS. Interestingly, cholesterol biosynthesis was increased in spite of the overall downregulation of genes in the cholesterol biosynthetic pathway. This puzzling phenomenon might be explained by an increase in HMG-CoA reductase activity, the rate-limiting enzyme in cholesterol biosynthesis. The induction of HMG-CoA reductase activity should be through its post-transcriptional regulations; both translation and degradation of HMG-CoA reductase protein are subject to feedback regulation by nonsterol mevalonate metabolites, as mentioned above. In the state of overwhelmingly increased activity of SS, most of the mevalonate metabolites may be utilized to produce squalene, leaving little substrates for nonsterol pathways such as geranyl diphosphate and farnesyl diphosphate. Under this condition, it is expected that translation of HMG-CoA reductase is increased and that its proteosomal ER degradation is suppressed, because farnesol (35, 36) and/or granylgeraniol (6) stimulate degradation of this enzyme. To verify this possibility, we need to examine the protein stability of HMG-CoA reductase and the cellular contents of isoprenoids. Unfortunately, we failed to detect HMG-CoA reductase protein in the liver membrane fractions by Western blot analysis, although we followed the established protocol and used two different

antibodies against HMG-CoA reductase. Our standard diet containing 0.075% of cholesterol might suppress the HMG-CoA reductase protein to a level below the sensitivity (37). A similar deficiency of mevalonate metabolites may underlie the marked upregulation of HMG-CoA reductase in cells from mevalonate kinase-deficient patients, where HMG-CoA reductase activity is increased by 6-fold despite the absence of the increases in its expression level (38). In addition to the substrate pool size of isoprenoids in the cholesterol biosynthetic pathway, flux to the isoprenoid pathway might be regulated by a separate isoprenoid transport network that selectively extracts some of these compounds and distributes them to other synthetic enzymes.

There are two potential explanations for the hypercholesterolemia in mice infected with Ad-SS: *i*) secretion of cholesterol-rich VLDL and *ii*) defective plasma clearance of LDL. Involvement of the secretion of cholesterol-rich VLDL is supported by the following findings: *1*) LDL-cholesterol was increased even in the LDLR knockout mice in which the LDL clearance was maximally suppressed (Fig. 4B). *2*) Cholesterol-rich VLDL was accumulated in the plasma of mice after the intravenous injection of Triton WR1339 (Fig. 5B). *3*) Hepatic ACAT activity, which is tightly associated with VLDL secretion (39–41), was increased. Supporting this, an in vitro study using McARH7777 cells showed that the secretion of cholesterol and fatty acids into the medium was increased when the cells overexpressed SS (Fig. 6). In this regard, it is interesting to note that some SS inhibitors, but not statins, inhibit VLDL secretion from the liver (17, 34, 42). These considerations suggest the intriguing possibility that nonsterol mevalonate metabolites, for example, farnesol, or newly synthesized cholesterol regulate VLDL secretion (42); this awaits further investigation. Defective LDL clearance may also contribute to the development of hypercholesterolemia, because the mRNA expression of the LDLR gene is downregulated (Table 1). The downregulation of the LDLR gene might result from the feedback regulation by the increased cholesterol biosynthesis. Consistently, SS inhibitors stimulate the LDLR activity (16, 17).

It is of note that cholesterol contents per weight of wet tissue did not significantly increase in the liver despite the increased cholesterol synthesis (Table 2). This resistance to cholesterol accumulation was not observed in transgenic mice overexpressing SREBP-1a, -1c, or -2 under the control of the phosphoenolpyruvate carboxykinase promoter in which cholesterol synthesis is stimulated by the overexpression of the active form of SREBPs and which exhibit massive accumulation of cholesterol in the liver (43–45). One explanation for this may be that the degree of the increase in cholesterol synthesis was not large enough to achieve a detectable buildup of cholesterol in the liver, possibly because the time span (7 days) was not long enough. An increased cholesterol flux into the lipoprotein assembly without an increased hepatic uptake may be another explanation. SREBP may promote the transcription of genes that participate in lipid droplet formation, rather than genes involved in VLDL secretion. A third possibility is that cholesterol is efficiently eliminated out of the liver into the bile in compensation for the increased synthesis, although the expression of genes responsible for this pathway, such as cholesterol 7α-hydroxylase, was not significantly changed (Table 1). A final but most interesting possibility is that newly synthesized cholesterol may be utilized for the plasma membranes of dividing cells. The liver was heavier, with an increased number of cells positive for Ki-67, after infection with Ad-SS (Table 2, Fig. 3), indicating that the hepatocytes were in a hyperproliferative state. Although the precise mechanisms are currently unknown, changes in the expression of Ras and Ras-related proteins (46) or in the cholesterol content of caveolae (47) may be intriguing possibilities.

The present study shows that selective upregulation of SS may lead to hypercholesterolemia. Mutations in the SS gene that confer stimulation of enzymatic activity may underlie some forms of hypercholesterolemia. In combination with liver-specific knockout of SS, which is being generated in this lab, manipulation of hepatic SS activity should provide the basis for understanding the complex regulatory mechanisms in the cholesterol biosynthetic pathway and for developing novel therapeutic modalities for hyperlipoproteinemia.

We thank Drs. Y. K. Ho, Michael S. Brown, and Joseph L. Goldstein for the generous gift of the antibody against HMG-CoA reductase, Prof. Yusuke Furukawa for discussion, and Mika Hayashi for technical assistance. This work was supported in part by a grant-in-aid for scientific research from the Ministry of Education, Science and Culture.

REFERENCES

1. Goldstein, J. L., and M. S. Brown. 1990. Regulation of the mevalonate pathway. *Nature.* **343:** 425–430.
2. Brown, M. S., J. Ye, R. B. Rawson, and J. L. Goldstein. 2000. Regulated intramembrane proteolysis: a control mechanism conserved from bacteria to humans. *Cell.* **100:** 391–398.
3. Nakanishi, M., J. L. Goldstein, and M. S. Brown. 1988. Multivalent control of 3-hydroxy-3-methylglutaryl coenzyme A reductase. Mevalonate-derived product inhibits translation of mRNA and accelerates degradation of enzyme. *J. Biol. Chem.* **263:** 8929–8937.
4. Roitelman, J., and R. D. Simoni. 1992. Distinct sterol and nonsterol signals for the regulated degradation of 3-hydroxy-3-methylglutaryl-CoA reductase. *J. Biol. Chem.* **267:** 25264–25273.
5. Inoue, S., and R. D. Simoni. 1992. 3-Hydroxy-3-methylglutaryl-coenzyme A reductase and T cell receptor alpha subunit are differentially degraded in the endoplasmic reticulum. *J. Biol. Chem.* **267:** 9080–9086.
6. Sever, N., B. L. Song, D. Yabe, J. L. Goldstein, M. S. Brown, and R. A. DeBose-Boyd. 2003. Insig-dependent ubiquitination and degradation of mammalian 3-hydroxy-3-methylglutaryl-CoA reductase stimulated by sterols and geranylgeraniol. *J. Biol. Chem.* **278:** 52479–52490.
7. Sever, N., T. Yang, M. S. Brown, J. L. Goldstein, and R. A. DeBose-Boyd. 2003. Accelerated degradation of HMG CoA reductase mediated by binding of insig-1 to its sterol-sensing domain. *Mol. Cell.* **11:** 25–33.
8. Grundy, S. M., J. I. Cleeman, C. N. Merz, H. B. Brewer, Jr., L. T. Clark, D. B. Hunninghake, R. C. Pasternak, S. C. Smith, Jr., and N. J. Stone. 2004. Implications of recent clinical trials for the National Cholesterol Education Program Adult Treatment Panel III guidelines. *Arterioscler. Thromb. Vasc. Biol.* **24:** e149–e161.
9. Kita, T., M. S. Brown, and J. L. Goldstein. 1980. Feedback regulation of 3-hydroxy-3-methylglutaryl coenzyme A reductase in livers of mice treated with mevinolin, a competitive inhibitor of the reductase. *J. Clin. Invest.* **66:** 1094–1100.

10. Thompson, P. D., P. Clarkson, and R. H. Karas. 2003. Statin-associated myopathy. *J. Am. Med. Assoc.* **289:** 1681–1690.
11. Shechter, I., E. Klinger, M. L. Rucker, R. G. Engstrom, J. A. Spirito, M. A. Islam, B. R. Boettcher, and D. B. Weinstein. 1992. Solubilization, purification, and characterization of a truncated form of rat hepatic squalene synthetase. *J. Biol. Chem.* **267:** 8628–8635.
12. McKenzie, T. L., G. Jiang, J. R. Straubhaar, D. G. Conrad, and I. Shechter. 1992. Molecular cloning, expression, and characterization of the cDNA for the rat hepatic squalene synthase. *J. Biol. Chem.* **267:** 21368–21374.
13. Guan, G., P. H. Dai, T. F. Osborne, J. B. Kim, and I. Shechter. 1997. Multiple sequence elements are involved in the transcriptional regulation of the human squalene synthase gene. *J. Biol. Chem.* **272:** 10295–10302.
14. Memon, R. A., I. Shechter, A. H. Moser, J. K. Shigenaga, C. Grunfeld, and K. R. Feingold. 1997. Endotoxin, tumor necrosis factor, and interleukin-1 decrease hepatic squalene synthase activity, protein, and mRNA levels in Syrian hamsters. *J. Lipid Res.* **38:** 1620–1629.
15. Baxter, A., B. J. Fitzgerald, J. L. Hutson, A. D. McCarthy, J. M. Motteram, B. C. Ross, M. Sapra, M. A. Snowden, N. S. Watson, R. J. Williams, et al. 1992. Squalestatin 1, a potent inhibitor of squalene synthase, which lowers serum cholesterol in vivo. *J. Biol. Chem.* **267:** 11705–11708.
16. Hiyoshi, H., M. Yanagimachi, M. Ito, I. Ohtsuka, I. Yoshida, T. Saeki, and H. Tanaka. 2000. Effect of ER-27856, a novel squalene synthase inhibitor, on plasma cholesterol in rhesus monkeys: comparison with 3-hydroxy-3-methylglutaryl-CoA reductase inhibitors. *J. Lipid Res.* **41:** 1136–1144.
17. Nishimoto, T., Y. Amano, R. Tozawa, E. Ishikawa, Y. Imura, H. Yukimasa, and Y. Sugiyama. 2003. Lipid-lowering properties of TAK-475, a squalene synthase inhibitor, in vivo and in vitro. *Br. J. Pharmacol.* **139:** 911–918.
18. Tozawa, R., S. Ishibashi, J. Osuga, H. Yagyu, T. Oka, Z. Chen, K. Ohashi, S. Perrey, F. Shionoiri, N. Yahagi, et al. 1999. Embryonic lethality and defective neural tube closure in mice lacking squalene synthase. *J. Biol. Chem.* **274:** 30843–30848.
19. Ohashi, K., J. Osuga, R. Tozawa, T. Kitamine, H. Yagyu, M. Sekiya, S. Tomita, H. Okazaki, Y. Tamura, N. Yahagi, et al. 2003. Early embryonic lethality caused by targeted disruption of the 3-hydroxy-3-methylglutaryl-CoA reductase gene. *J. Biol. Chem.* **278:** 42936–42941.
20. Tsukamoto, K., P. Smith, J. M. Glick, and D. J. Rader. 1997. Liver-directed gene transfer and prolonged expression of three major human ApoE isoforms in ApoE-deficient mice. *J. Clin. Invest.* **100:** 107–114.
21. Okazaki, H., J. Osuga, K. Tsukamoto, N. Isoo, T. Kitamine, Y. Tamura, S. Tomita, M. Sekiya, N. Yahagi, Y. Iizuka, et al. 2002. Elimination of cholesterol ester from macrophage foam cells by adenovirus-mediated gene transfer of hormone-sensitive lipase. *J. Biol. Chem.* **277:** 31893–31899.
22. Ishibashi, S., M. S. Brown, J. L. Goldstein, R. D. Gerard, R. E. Hammer, and J. Herz. 1993. Hypercholesterolemia in low density lipoprotein receptor knockout mice and its reversal by adenovirus-mediated gene delivery. *J. Clin. Invest.* **92:** 883–893.
23. Yang, J., J. L. Goldstein, R. E. Hammer, Y. A. Moon, M. S. Brown, and J. D. Horton. 2001. Decreased lipid synthesis in livers of mice with disrupted Site-1 protease gene. *Proc. Natl. Acad. Sci. USA.* **98:** 13607–13612.
24. Cohen, L. H., A. M. Griffioen, R. J. Wanders, C. W. Van Roermund, C. M. Huysmans, and H. M. Princen. 1986. Regulation of squalene synthetase activity in rat liver: elevation by cholestyramine, but no diurnal variation. *Biochem. Biophys. Res. Commun.* **138:** 335–341.
25. Yagyu, H., T. Kitamine, J. Osuga, R. Tozawa, Z. Chen, Y. Kaji, T. Oka, S. Perrey, Y. Tamura, K. Ohashi, et al. 2000. Absence of ACAT-1 attenuates atherosclerosis but causes dry eye and cutaneous xanthomatosis in mice with congenital hyperlipidemia. *J. Biol. Chem.* **275:** 21324–21330.
26. Folch, J., M. Lees, and G. H. Sloane Stanley. 1957. A simple method for the isolation and purification of total lipides from animal tissues. *J. Biol. Chem.* **226:** 497–509.
27. Heider, J. G., and R. L. Boyett. 1978. The picomole determination of free and total cholesterol in cells in culture. *J. Lipid Res.* **19:** 514–518.
28. Eisele, B., R. Budzinski, P. Muller, R. Maier, and M. Mark. 1997. Effects of a novel 2,3-oxidosqualene cyclase inhibitor on cholesterol biosynthesis and lipid metabolism in vivo. *J. Lipid Res.* **38:** 564–575.
29. Horton, J. D., H. Shimano, R. L. Hamilton, M. S. Brown, and J. L. Goldstein. 1999. Disruption of LDL receptor gene in transgenic SREBP-1a mice unmasks hyperlipidemia resulting from production of lipid-rich VLDL. *J. Clin. Invest.* **103:** 1067–1076.
30. Shibata, N., M. Arita, Y. Misaki, N. Dohmae, K. Takio, T. Ono, K. Inoue, and H. Arai. 2001. Supernatant protein factor, which stimulates the conversion of squalene to lanosterol, is a cytosolic squalene transfer protein and enhances cholesterol biosynthesis. *Proc. Natl. Acad. Sci. USA.* **98:** 2244–2249.
31. Aalto-Setala, K., E. A. Fisher, X. Chen, T. Chajek-Shaul, T. Hayek, R. Zechner, A. Walsh, R. Ramakrishnan, H. N. Ginsberg, and J. L. Breslow. 1992. Mechanism of hypertriglyceridemia in human apolipoprotein (apo) CIII transgenic mice. Diminished very low density lipoprotein fractional catabolic rate associated with increased apo CIII and reduced apo E on the particles. *J. Clin. Invest.* **90:** 1889–1900.
32. Dietschy, J. M., and D. K. Spady. 1984. Measurement of rates of cholesterol synthesis using tritiated water. *J. Lipid Res.* **25:** 1469–1476.
33. Gerdes, J., U. Schwab, H. Lemke, and H. Stein. 1983. Production of a mouse monoclonal antibody reactive with a human nuclear antigen associated with cell proliferation. *Int. J. Cancer.* **31:** 13–20.
34. Ugawa, T., H. Kakuta, H. Moritani, O. Inagaki, and H. Shikama. 2003. YM-53601, a novel squalene synthase inhibitor, suppresses lipogenic biosynthesis and lipid secretion in rodents. *Br. J. Pharmacol.* **139:** 140–146.
35. Correll, C. C., L. Ng, and P. A. Edwards. 1994. Identification of farnesol as the non-sterol derivative of mevalonic acid required for the accelerated degradation of 3-hydroxy-3-methylglutaryl-coenzyme A reductase. *J. Biol. Chem.* **269:** 17390–17393.
36. Meigs, T. E., and R. D. Simoni. 1997. Farnesol as a regulator of HMG-CoA reductase degradation: characterization and role of farnesyl pyrophosphatase. *Arch. Biochem. Biophys.* **345:** 1–9.
37. Engelking, L. J., G. Liang, R. E. Hammer, K. Takaishi, H. Kuriyama, B. M. Evers, W. P. Li, J. D. Horton, J. L. Goldstein, and M. S. Brown. 2005. Schoenheimer effect explained—feedback regulation of cholesterol synthesis in mice mediated by Insig proteins. *J. Clin. Invest.* **115:** 2489–2498.
38. Houten, S. M., M. S. Schneiders, R. J. Wanders, and H. R. Waterham. 2003. Regulation of isoprenoid/cholesterol biosynthesis in cells from mevalonate kinase-deficient patients. *J. Biol. Chem.* **278:** 5736–5743.
39. Huff, M. W., D. E. Telford, P. H. Barrett, J. T. Billheimer, and P. J. Gillies. 1994. Inhibition of hepatic ACAT decreases ApoB secretion in miniature pigs fed a cholesterol-free diet. *Arterioscler. Thromb.* **14:** 1498–1508.
40. Musanti, R., L. Giorgini, P. P. Lovisolo, A. Pirillo, A. Chiari, and G. Ghiselli. 1996. Inhibition of acyl-CoA: cholesterol acyltransferase decreases apolipoprotein B-100-containing lipoprotein secretion from HepG2 cells. *J. Lipid Res.* **37:** 1–14.
41. Spady, D. K., M. N. Willard, and R. S. Meidell. 2000. Role of acyl-coenzyme A:cholesterol acyltransferase-1 in the control of hepatic very low density lipoprotein secretion and low density lipoprotein receptor expression in the mouse and hamster. *J. Biol. Chem.* **275:** 27005–27012.
42. Hiyoshi, H., M. Yanagimachi, M. Ito, N. Yasuda, T. Okada, H. Ikuta, D. Shinmyo, K. Tanaka, N. Kurusu, I. Yoshida, et al. 2003. Squalene synthase inhibitors suppress triglyceride biosynthesis through the farnesol pathway in rat hepatocytes. *J. Lipid Res.* **44:** 128–135.
43. Shimano, H., J. D. Horton, R. E. Hammer, I. Shimomura, M. S. Brown, and J. L. Goldstein. 1996. Overproduction of cholesterol and fatty acids causes massive liver enlargement in transgenic mice expressing truncated SREBP-1a. *J. Clin. Invest.* **98:** 1575–1584.
44. Shimano, H., J. D. Horton, I. Shimomura, R. E. Hammer, M. S. Brown, and J. L. Goldstein. 1997. Isoform 1c of sterol regulatory element binding protein is less active than isoform 1a in livers of transgenic mice and in cultured cells. *J. Clin. Invest.* **99:** 846–854.
45. Horton, J. D., I. Shimomura, M. S. Brown, R. E. Hammer, J. L. Goldstein, and H. Shimano. 1998. Activation of cholesterol synthesis in preference to fatty acid synthesis in liver and adipose tissue of transgenic mice overproducing sterol regulatory element-binding protein-2. *J. Clin. Invest.* **101:** 2331–2339.
46. Holstein, S. A., C. L. Wohlford-Lenane, and R. J. Hohl. 2002. Consequences of mevalonate depletion. Differential transcriptional, translational, and post-translational up-regulation of Ras, Rap1a, RhoA, and RhoB. *J. Biol. Chem.* **277:** 10678–10682.
47. Razani, B., J. A. Engelman, X. B. Wang, W. Schubert, X. L. Zhang, C. B. Marks, F. Macaluso, R. G. Russell, M. Li, R. G. Pestell, et al. 2001. Caveolin-1 null mice are viable but show evidence of hyperproliferative and vascular abnormalities. *J. Biol. Chem.* **276:** 38121–38138.

Available online at www.sciencedirect.com
SCIENCE DIRECT
ELSEVIER
Diabetes Research and Clinical Practice 70 (2005) 183–192
DIABETES RESEARCH AND CLINICAL PRACTICE
www.elsevier.com/locate/diabres

Case report

Diabetic lipemia with eruptive xanthomatosis in a lean young female with apolipoprotein E4/4

Satoshi Shinozaki [a], Naoki Itabashi [a], Kumiko Rokkaku [a], Kenji Ichiki [a], Shoichiro Nagasaka [a,*], Koji Okada [a], Mitsuo Fujimoto [b], Mamitaro Ohtsuki [b], Shun Ishibashi [a]

[a] *Division of Endocrinology and Metabolism, Department of Medicine, Jichi Medical School, Yakushiji 3311-1, Minamikawachi, Tochigi 329-0498, Japan*
[b] *Division of Dermatology, Department of Medicine, Jichi Medical School, Yakushiji 3311-1, Minamikawachi, Tochigi 329-0498, Japan*

Received 18 October 2004; received in revised form 15 February 2005; accepted 3 March 2005
Available online 12 April 2005

Abstract

Eruptive xanthomas in adults are usually indicative of chylomicronemia. Although diabetes mellitus is the most common secondary cause of chylomicronemia, which is designated as diabetic lipemia, the clinical characteristics of diabetes with regard to development of xanthomas are not well defined. In this paper, we describe a young female who displayed eruptive xanthomas as an initial manifestation of diabetic lipemia. The patient was a 20-year-old female with a body mass index of 18.9 kg/m^2 and Marfanoid appearance. Her past history was unremarkable, except for patent ductus arteriosus and mild mental retardation. She was admitted to our division for eruptive xanthomas on the extremities and marked hyperglycemia (random glucose, 520 mg/dl) and hypertriglyceridemia (6880 mg/dl). She was diagnosed with Type 2 diabetes based on the positive family history of diabetes, residual secretory capacity of insulin, and absence of autoantibodies related to Type 1 diabetes. Based on the increase in the concentrations of both chylomicrons and very low density lipoproteins, type V hyperlipoproteinemia was diagnosed. After the initiation of insulin therapy, both hypertriglyceridemia and eruptive xanthomas subsided, without administering any hypolipidemic agents. Minimal model analysis of a frequently sampled intravenous glucose tolerance test revealed severe insulin resistance, despite the absence of obesity. Post-heparin lipoprotein lipase (LPL) activity was moderately decreased, and common mutations in the LPL gene were not demonstrated by genetic screening. The apolipoprotein E phenotype was E4/4, which is known to be associated with type V hyperlipoproteinemia. Hypoadiponectinemia of 1.7 μg/ml was also revealed, which may, in part, account for the insulin resistance and decreased LPL activity. In conclusion, the clustering of apolipoprotein E4/4 and hypoadiponectinemia, in addition to insulin resistance and poor glycemic control, might have resulted in hypertriglyceridemia with eruptive xanthomatosis in this subject.

Keywords: Diabetic lipemia; Hypertriglyceridemia; Chylomicronemia; Apolipoprotein E; Eruptive xanthoma; Insulin resistance; Adiponectin

* Corresponding author. Tel.: +81 285 58 7355; fax: +81 285 44 8143.
E-mail address: sngsk@jichi.ac.jp (S. Nagasaka).

0168-8227/$ – see front matter
doi:10.1016/j.diabres.2005.03.023

1. Introduction

Eruptive xanthomas in adults are usually indicative of chylomicronemia with triglyceride levels greater than 2000 mg/dl [1]. Genetic defects, such as lipoprotein lipase (LPL) deficiency, and/or secondary disturbances in the triglyceride metabolism can result in chylomicronemia. Although diabetes mellitus is the most common secondary cause of type V hyperlipoproteinemia, a type of chylomicronemia, few reports are available on the precise characteristics of the diabetic patients who display eruptive xanthomas and hypertriglyceridemia. In this paper, we report the case of a young female patient who displayed eruptive xanthomas as an initial manifestation of diabetes mellitus and hypertriglyceridemia. The peculiar characteristics of this patient included a Marfanoid appearance, severe insulin resistance, and hypoadiponectinemia, despite the absence of obesity and apolipoprotein E4/4 phenotype. In order to define the clinical characteristics of diabetic patients who display eruptive xanthomas, the relationship between eruptive xanthomas and diabetes mellitus was also investigated by reviewing the relevant literature.

2. Material and methods

2.1. Case report

The patient was a 20-year-old Japanese female with mild mental retardation. Her past history was unremarkable with the exception of a surgery for patent ductus arteriosus at the age of 10 years. At that time, the serum levels of total cholesterol and triglyceride were 141 and 74 mg/dl, respectively. She did not consume alcohol or tobacco. The family history revealed that her maternal grandfather, maternal aunt, and mother had diabetes mellitus. Her mother died of acute myocardial infarction at the age of 51 years; she had undergone hemodialysis for chronic renal failure due to diabetic nephropathy. She had also undergone bilateral lower limb amputations. The patient's father died of pancreatic cancer at the age of 47 years. Her elder brother had verbal disability and mental retardation. In these subjects, past history of hyperlipidemia was unremarkable, and data on plasma lipids were not available. There was no consanguineous marriage in this pedigree.

On December 28, 2001, the patient observed a number of yellow papules surrounded by moderate red halo spreading on the dorsal surface of both hands. Within a few days, these papules spread to the extensor surface of forearms, upper arms, and thighs. She complained of moderate pruritus on the dorsal surface of the hands, but was otherwise asymptomatic and had no abdominal pain. On investigating, a local physician detected marked hyperglycemia (random glucose of 520 mg/dl) and hyperlipidemia with serum triglyceride and total cholesterol levels of 6880 and 901 mg/dl, respectively. She was referred to the hospital for further evaluation and admitted to the author's division on January 10, 2002.

The patient's profile was as follows: height, 159.5 cm; weight, 48 kg; body mass index, 18.9 kg/m^2; and blood pressure, 128/90 mmHg. Diabetic retinopathy, lipemia retinalis, and ectopia lentis were not observed. Examination of the neck, chest, and abdomen revealed no abnormal findings, except for a scar on the chest. A cardiac echogram did not show any valvular or aortic abnormalities. Several non-confluent yellow papules, 2–5 mm in diameter, with erythematous halos, were observed on the dorsal surface of the hands, extensor surface of the forearms, upper arms, and thighs (Fig. 1). Similar lesions were not observed on the trunk and buttocks. The patellar and Achilles tendon reflexes and the sense of vibration in the legs were normal. The arm span was 163 cm, which was greater than her height. Arachnodactyly was observed; however, no extreme extensibility in the joints of the extremities was observed.

Routine laboratory examination (Table 1) revealed increased levels of fasting plasma glucose (FPG) and HbA_{1c} along with mildly elevated levels of ketone bodies and free fatty acid (FFA); however, blood gas analysis did not reveal metabolic acidosis. The serum total cholesterol and triglyceride levels were extremely increased, and an overnight incubation of her serum revealed the presence of chylomicrons. Serum high density lipoprotein (HDL) cholesterol level, measured by a homogenous assay (polyethylene glycol-modified enzyme/α-cyclodextrin sulfate assay, Kyowa Medex, Tokyo, Japan), was as high as 69 mg/dl despite severe hypertriglyceridemia. However, it is likely that the level was overestimated because this

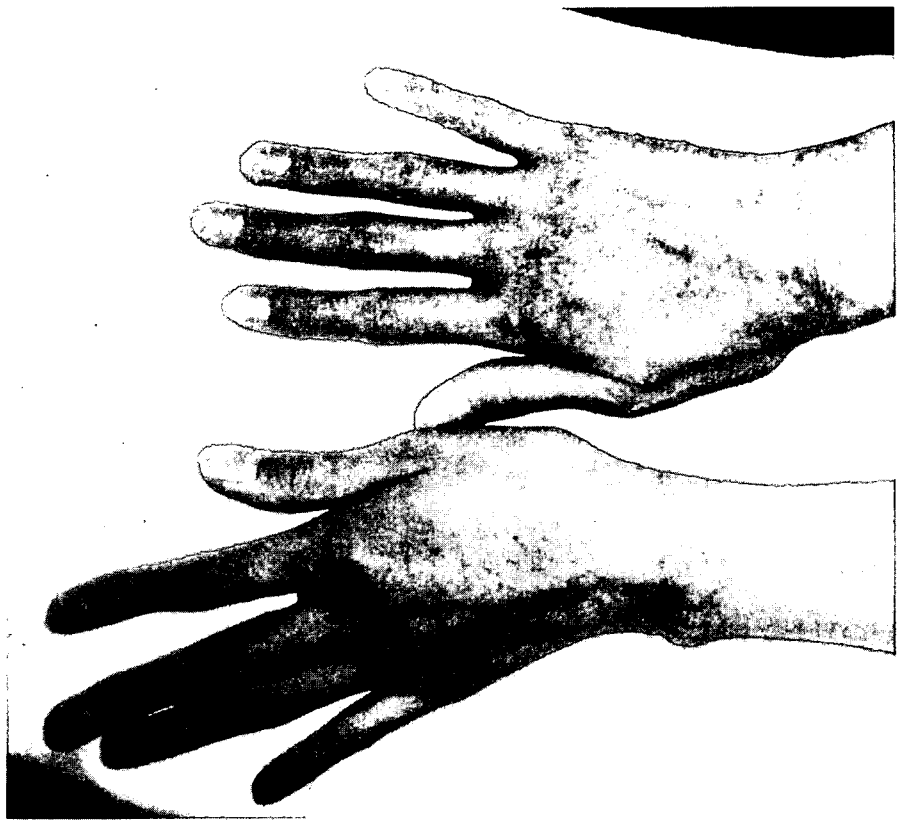

Fig. 1. Eruptive xanthomas on the dorsal surface of the hands. Note the presence of arachnodactyly.

assay has been shown to cross-react, in part, with the fractions of chylomicrons and very low density lipoprotein (VLDL) [2]. Serum amylase concentration was within the normal reference range, and no evidence of pancreatitis was observed on an abdominal echogram. Serum and urinary C-peptide levels were moderately decreased, and both anti-glutamic acid decarboxylase (GAD) and anti-insulinoma-associated protein 2 (IA-2) antibodies (measured using commercial RIA kits; Cosmic Corporation, Tokyo, Japan) were negative. Thyroid function tests revealed decreased levels of free T_3 and T_4, with normal TSH level; this was suggestive of a non-thyroidal illness.

On the next day after admission (Day 2), detailed analysis of serum lipids was performed (Table 2). Prior to these examinations, insulin was not administered. Quantification of serum total lipoproteins, measured by a heparin-$CaCl_2$ precipitation method (BLF "Eiken," Eiken Chemical, Tokyo, Japan), revealed a marked increase in chylomicrons and VLDL and a moderate increase in low density lipoprotein (LDL); this was indicative of type V hyperlipoproteinemia. Remnant-like lipoprotein particle cholesterol (RLP-C) level was also elevated. Apolipoprotein C2, C3, and E levels were markedly increased, and the apolipoprotein E phenotype was E4/4. Quantification of LPL mass, measured 10 min after an intravenous injection of heparin (30 U/kg body weight), revealed that it was within the normal reference range, and the post-heparin LPL activity was moderately decreased. Hepatic triglyceride lipase (HTGL) activity was within the normal reference range.

Regarding the adipocytokines, the serum leptin concentration of 5.5 ng/ml, measured by a radioimmunoassay kit (Linco Research Inc., St. Charles, MO), was appropriate for her BMI [3]. Serum tumor necrosis factor α level, measured by an enzyme-linked immunosorbent assay (ELISA) kit (Japan Immunor-

Table 1
General laboratory findings on admission

Urinalysis		Biochemistry		Endocrinology	
Protein	2+	TP	7.8 g/dl	Total ketone bodies	1462 μM
Sugar	3+	Albumin	4.5 g/dl	AcAc	232 μM
Urobilinogen	±	BUN	9 mg/dl	3-OHBA	1230 μM
Bilirubin	–	Cr	0.21 mg/dl	FFA	1.60 mEq/l
Ketone body	3+	UA	4.1 mg/dl		
Hematology		T-Bil	0.31 mg/dl	Serum C-peptide	
WBC	6500/μl	ALP	104 mU/ml	Fasting	0.9 ng/ml
RBC	419 × 10^4/μl	AST	8 mU/ml	Post-prandial	2.8 ng/ml
Hb	14.2 g/dl	ALT	4 mU/ml	Urine C-peptide	17.3 μg/day
Ht	37.7%	LDH	453 mU/ml		
Plt	12.5 × 10^4/μl	γ-GTP	39 mU/ml	Anti-GAD antibody	<0.3 U/ml
Blood gas analysis		Amylase	57 mU/ml	IA-2 antibody	<0.1 U/ml
pH	7.382	T-Chol	953 mg/dl		
P_{CO_2}	43.3 mmHg	HDL-Chol	69 mg/dl	TSH	2.10 μU/ml
P_{O_2}	73.5 mmHg	TG	4538 mg/dl	Free T_3	1.14 pg/ml
HCO_3^-	25.2 mmol/l	FPG	350 mg/dl	Free T_4	0.61 ng/dl
BE	0.0 mmol/l	HbA_{1c}	15.7%		

esearch Laboratories, Takasaki, Japan), was less than 5 pg/ml. Serum high-molecular weight adiponectin concentration, measured by a specific ELISA kit (Fujirebio, Tokyo, Japan), was as low as 1.7 μg/ml as compared to 9.0 ± 6.1 μg/ml in the more obese Type 2 diabetic female patients (n = 12; BMI, 22.0 ± 4.0 kg/m^2; mean ± S.D.).

Histopathological examination of the biopsy specimen of the eruptions on the extensor surface of the forearm was consistent with eruptive xanthoma, showing multiple infiltrating foamy histiocytes (Fig. 2).

After the analysis of lipid abnormalities, insulin therapy was introduced, and the dose of insulin was gradually increased (Fig. 3). Finally, a total of 42 units of premixed insulin (Penfill-30R, Novo Nordisk Pharma, Tokyo, Japan) was administered daily; this decreased the pre- and post-prandial glucose levels to

Table 2
Detailed analysis of serum lipids

	Day 2 (on admission)	Day 23	Normal range
Chylomicron	6350	84	<30 mg/dl
VLDL	3080	436	<210 mg/dl
LDL	800	995	190–580 mg/dl
RLP-C	606.9	ND	<7.5 mg/dl
Lp (a)	3	ND	<40 mg/dl
Apolipoprotein A1	99	89	126–165 mg/dl
Apolipoprotein A2	21.4	20.1	24.6–33.3 mg/dl
Apoipoprotein B	218	165	66–101 mg/dl
Apolipoprotein C2	78.8	8.4	1.5–3.8 mg/dl
Apolipoprotein C3	115.5	12.8	5.4–9.0 mg/dl
Apolipoprotein E	57.4	6.8	2.8–4.6 mg/dl
Apolipoprotein E phenotype	4/4		
LPL mass	207	ND	164–284 ng/ml
LPL activity	0.145	ND	0.166–0.226 μmol/ml min
HTGL activity	0.255	ND	0.158–0.530 μmol/ml min

ND: not determined.

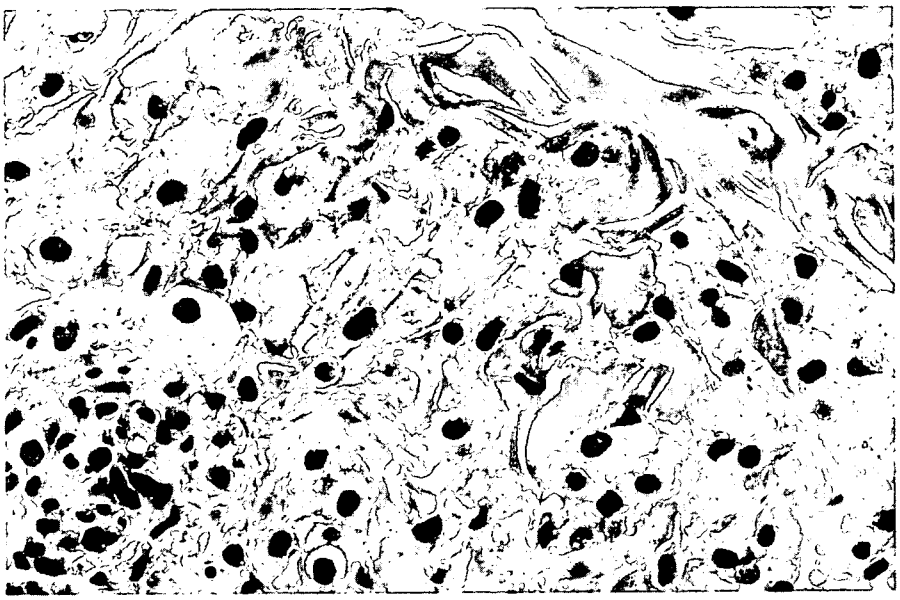

Fig. 2. Histopathology of the biopsy specimen of eruptive xanthoma (H&E staining, ×400 in original magnification). Multiple foamy histiocytes are seen throughout the dermis. A majority of these cells are mononuclear, and the Touton type giant cells are absent.

less than 200 mg/dl. Along with the improvement in glycemic control, serum levels of triglyceride and total cholesterol rapidly decreased without the administration of any hypolipidemic agents. Simultaneously, skin eruptions gradually disappeared at 1 month after the admission. On day 23, serum concentrations of chylomicrons; VLDL; apolipoprotein C2, C3, and E were restored to their normal reference ranges (Table 2), whereas the serum triglyceride and total cholesterol concentrations were 254 and 291 mg/dl, respectively. At the time of discharge (day 41), serum levels of triglyceride, total, and HDL cholesterol were 88, 169, and 31 mg/dl, respectively.

After the achievement of good glycemic control, an insulin-modified frequently sampled intravenous glucose tolerance test was performed as described

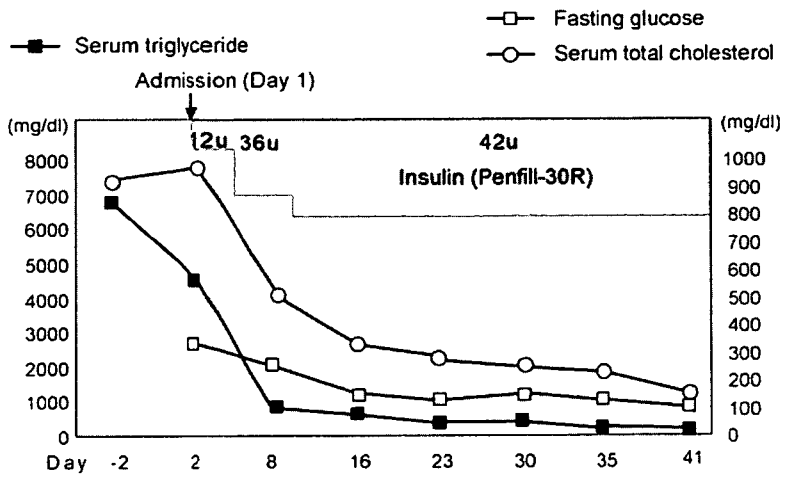

Fig. 3. The levels of fasting glucose, serum triglyceride, and total cholesterol of the patient during the study.

previously [4]. Acute insulin response to glucose within 10 min after the glucose bolus was markedly decreased, that is, 14.3 [(μU/ml) 10 min] in the patient, whereas it was 165 ± 51 [(μU/ml) 10 min, mean ± S.E.] in the control subjects [5]. Minimal model analysis of plasma glucose and insulin kinetics yielded a zero insulin sensitivity index, suggesting severe insulin resistance even after the correction of hyperglycemia [6]. Glucose effectiveness (0.0153/min), that is, effects of glucose per se to normalize its own concentration, was also moderately decreased as compared to that in the control subjects (0.0203 ± 0.0022/min) [5].

After obtaining the patient's written informed consent, 22 mutations in the LPL gene, which have been demonstrated in the Japanese population (W-14X, N43S, Int2 + 1G/A, Y61X, G105R, G154V, G188E, I194T, V200A, D204E, A221del, C239X, R243C, R243H, A261T, F270L, C278R, N291del, S323C, A334T, W382X, and Int8 + 2T/C) were screened by Invader assay at the BML laboratory (http://www.bml.co.jp/genome/invadertech.html). All the mutations were shown to be present in the normal homozygous states.

3. Discussion

The present case displayed typical eruptive xanthomas, proven by histopathological analysis, associated with type V hyperlipoproteinemia and diabetes mellitus. Since eruptive xanthomas subsided with the achievement of glycemic control by insulin administration, the hyperlipidemia present in the subject can be regarded as the so-called diabetic lipemia [7]. Regarding the etiology of diabetes mellitus, the possibility of Type 1 diabetes mellitus was unlikely because of a strong family history of diabetes, demonstration of moderately decreased insulin secretion by C-peptide measurement, and absence of autoantibodies related to Type 1 diabetes. Although the patient was not obese, the dose of insulin required to correct hyperglycemia was not moderate (0.88 unit/kg), and minimal model analysis of an intravenous glucose tolerance test revealed severe insulin resistance. There might be some possibility of the existence of maturity-onset diabetes of the young (MODY) in this family because of the clustering of diabetic subjects and younger age of onset of the disease in the proband. However, it appears unlikely that the proband may have any known MODY mutations because subjects with such MODY mutations usually have deficient insulin secretion, but not insulin resistance [8]. Finally, after considering the various factors, she was diagnosed as having Type 2 diabetes.

In the present case, although the exact pathogenesis of insulin resistance remains to be clarified, measurements of several adipocytokines revealed the presence of hypoadiponectinemia. Adiponectin, an adipose tissue-derived circulating protein, has insulin-sensitizing and anti-atherogenic properties [9]. Circulating concentrations of adiponectin are known to be decreased in obesity and Type 2 diabetes [10], and the decrease in adiponectin concentration is considered to be one of the pathogenic factors for insulin resistance in Type 2 diabetic patients [11]. Since this lean patient showed markedly decreased adiponectin levels as compared to more obese Type 2 diabetic females, hypoadiponectinemia is likely to play a role in the evolution of insulin resistance.

In the present case, the etiology of type V hyperlipoproteinemia appears to be multifactorial. First, the presence of marked hyperglycemia and ketosis, on admission, suggests deficient insulin action; this could be associated with a transient deficiency of LPL, a key enzyme of triglyceride catabolism, and increased lipolysis leading to VLDL overproduction [12]. This assumption is supported by the fact that the achievement of glycemic control by insulin therapy resulted in the normalization of hyperlipidemia. The decrease in insulin action can be due to defective insulin secretion, insulin resistance, or both. In the present case, minimal model analysis revealed a zero insulin sensitivity index [6] even after the hyperglycemia was corrected and glucose toxicity was removed. Therefore, the insulin resistance might have been much greater on admission and, presumably, might have contributed to the decreased insulin action to a great extent. Independent of the association with insulin resistance, hypoadiponectinemia has been recently shown to be directly associated with decreased post-heparin LPL activity [13]. Therefore, hypoadiponectinemia could also account for the decreased LPL activity as well as the pathogenesis of insulin resistance.

It is well recognized that the degree of hypertriglyceridemia is variable among diabetic subjects who have marked hyperglycemia. Therefore, some

Table 3
Eruptive xanthoma and diabetes mellitus (literature review)

Onset age of xanthoma (years)	Sex	Onset age of diabetes (years)	Type of diabetes	BMI (kg/m^2)	Family history of diabetes	Fasting glucose (mg/dl)	HbA_{1c} (%)	TG (mg/dl)	T-Chol (mg/dl)	Type of hyperlipidemia	Reference
20	Male	17	NR	NR	+	300	NR	1525	839	V	[23]
29	Male	27	2	31.1	+	365	NR	1129	596	IV	[24]
24	Male	21	2	34.3	+	200	NR	1969	535	V	[25]
19	Female	19	2	18.2	–	185	NR	1040	366	III	[26]
35	Male	25	2 (probable)	36.2	+	211	10.4	4188	888	V	[27]
30	Male	27	2 (probable)	28	+	349	NR	6640	780	V	[28]
35	Male	28	2 (probable)	34.6	–	261	8.6	3165	402	V	[29]
15	Female	13	2	32	+	283	15.5	6230	682	V	[30]
35	Male	34	2	27.1	+	245	NR	4300	1095	V	[31]
43	Male	43	2 (probable)	26.6	+	210	10.2	2008	655	V	[32]
45	Female	40	2	27.6	–	134	8.6	2572	558	IV	[33]
17	Female	13	2	NR	–	322	11	3275	465	I	[34]
43	Male	39	2	31.9	+	242	8.7	2901	402	V	[35]
40	Male	40	2	NR	+	398	NR	11700	1067	V	[36]
28	Female	15	2	27	+	171	11.5	2785	750	IV	[37]
38	Male	38	2	NR	NR	241	13.4	8869	1268	V	[38]
20	Female	20	2	18.9	+	350	15.7	6880	901	V	Present case

NR: not recorded.

genetic and environmental susceptibility to hypertriglyceridemia should also be considered [14]. The contribution of drugs, such as corticosteroids or estrogen, alcohol consumption, and hypothyroidism, to causing hypertriglyceridemia appear unlikely based on the history and laboratory findings. Apolipoprotein C2 deficiency, which can result in type V hyperlipoproteinemia, was not observed. Although compound heterozygous two mutations in the LPL gene were demonstrated in a subject with diabetic ketoacidosis and severe hypertriglyceridemia [15], the present case did not have any known LPL mutations, seen in the Japanese population, both in heterozygous and homozygous manners. However, the presence of very rare mutations cannot be completely ruled out at present.

The subject showed apolipoprotein E phenotype of E4/4; this phenotype is associated with an increased risk of coronary heart disease [16], vascular dementia [17], and late-onset familial Alzheimer disease [18]. With regard to its association with hyperlipidemia, Ghiselli et al. [19] first reported the increased prevalence of apolipoprotein E4 phenotype in type V hyperlipoproteinemia. According to their results, approximately one-third of the patients with type V hyperlipoproteinemia were homozygous for the E4 allele. Supporting this finding, apolipoprotein E4 gene frequency was also found to be increased in obese subjects with hypertriglyceridemia [20]. Increased intestinal cholesterol absorption [21] and/or postprandial hyperlipidemia [22] have been postulated to explain this association.

Table 3 summarizes the clinical characteristics of 17 subjects (11 males and 6 females, including the present case) who had diabetes mellitus and eruptive xanthoma; they were found by literature review [23–38]. With the exception of a few subjects, eruptive xanthomas were noted at the time of initial diagnosis of diabetes or within a few years of the diagnosis. Most subjects were diagnosed as having Type 2 diabetes, and the age of onset of diabetes was less than 40 years in 14 (82%) of the 17 subjects. Consistent with Type 2 diabetes, obesity with BMI greater than 25 kg/m^2 and positive family history of diabetes were present in most of the subjects. The levels of fasting glucose, HbA_{1c}, serum triglyceride, and total cholesterol were markedly elevated, and 12 subjects were diagnosed with type V hyperlipoproteinemia (71%). Obesity and poor glycemic control generally indicates the presence of insulin resistance, which results in decreased LPL activity and increased VLDL production. Elevated HbA_{1c} levels suggest that hyperglycemia may have persisted for at least 1 or 2 months, and eruptive xanthomas may develop during these periods with persistent hypertriglyceridemia. Among all the reviews, we did not observe any case report that described marked hypertriglyceridemia and eruptive xanthomas in Type 1 diabetic subjects. The duration of hypertriglyceridemia may not have been long enough for the development of eruptive xanthomas in case of severe insulin deficiency of Type 1 diabetes.

The present case showed a few Marfanoid features, such as arachnodactyly and elongated arm span; however, no abnormalities in the lens and cardiovascular system were observed, and none of the family members showed typical Marfanoid features. Therefore, at present, making a definite diagnosis of Marfan syndrome appeared to be difficult [39]. A case report of a female with Marfan syndrome and Type 1 diabetes has been described previously [40]; however, the relationship between Marfan syndrome and Type 2 diabetes remains unknown.

In conclusion, this paper has reported a case of a female patient with early onset Type 2 diabetes who displayed marked hyperglycemia, hypertriglyceridemia (type V hyperlipoproteinemia) and eruptive xanthomas. The patient was also characterized by Marfanoid appearance, presence of insulin resistance, and hypoadiponectinemia, despite the absence of obesity. It appeared unlikely that the LPL gene mutations contributed to hypertriglyceridemia. The clustering of apolipoprotein E4/4 and hypoadiponectinemia, in addition to insulin resistance and poor glycemic control, might have resulted in hypertriglyceridemia with eruptive xanthomatosis in this subject.

Acknowledgments

We are indebted to Dr. Nobuyuki Kanai (Department of Pathology, Jichi Medical School) for his contribution to the histopathological analysis of the biopsy specimen of eruptive xanthoma, and to Mr. Takeo Sawada (Department of Clinical Laboratory, Jichi Medical School) for his contribution to the lipid analysis.

References

[1] R.H. Champion, J.L. Burton, D.A. Burns, S.M. Breathnach, Metabolic and nutritional disorders, in: Textbook of Dermatology, sixth ed., Blackwell Science, Oxford, UK, 1998, pp. 2577–2678.

[2] Y. Kayamori, M. Nasu, T. Matsumoto, I. Kakutani, S. Fujita, Y. Katayama, et al. Evaluation of five homogenous methods for measuring high-density lipoprotein cholesterol compared with ultracentrifugation method, J Anal Bio-Sci 23 (2000) 225–232 (in Japanese, Abstract in English).

[3] S. Nagasaka, S. Ishikawa, T. Nakamura, A. Kawakami, K. Rokkaku, H. Hayashi, et al. Association of endogenous insulin secretion and mode of therapy with body fat and serum leptin levels in diabetic subjects, Metabolism 47 (1998) 1391–1396.

[4] A. Taniguchi, Y. Nakai, M. Fukushima, H. Kawamura, H. Imura, I. Nagata, et al. Pathogenic factors responsible for glucose intolerance in patients with NIDDM, Diabetes 41 (1992) 1540–1546.

[5] S. Nagasaka, K. Tokuyama, I. Kusaka, H. Hayashi, K. Rokkaku, T. Nakamura, et al. Endogenous glucose production and glucose effectiveness in Type 2 diabetic subjects derived from stable-labeled minimal model approach, Diabetes 48 (1999) 1054–1060.

[6] S.M. Haffner, R. D'Agostino Jr., A. Festa, R.N. Bergman, L. Mykkanen, A. Karter, et al. Low insulin sensitivity (Si = 0) in diabetic and nondiabetic subjects in the Insulin Resistance Atherosclerosis Study, Diabetes Care 26 (2003) 2796–2803.

[7] J.D. Bagdade, E.L. Bierman, D. Porte Jr., Diabetic lipemia—a form of acquired fat-induced lipemia, N. Engl. J. Med. 276 (1967) 427–433.

[8] S.S. Fajans, G.I. Bell, K.S. Polonsky, Molecular mechanisms and clinical pathophysiology of maturity-onset diabetes of the young, N. Engl. J. Med. 345 (2001) 971–980.

[9] M. Chandran, T. Ciaraldi, S.A. Phillips, R.R. Henry, Adiponectin: more than just another fat cell hormone? Diabetes Care 26 (2003) 2442–2450.

[10] K. Hotta, T. Funahashi, Y. Arita, M. Takahashi, M. Matsuda, Y. Okamoto, et al. Plasma concentrations of a novel, adipose-specific protein, adiponectin, in Type 2 diabetic patients, Arterioscler. Thromb. Vasc. Biol. 20 (2000) 1595–1599.

[11] T. Yatagai, S. Nagasaka, A. Taniguchi, M. Fukushima, T. Nakamura, A. Kuroe, et al. Hypoadiponectinemia is associated with visceral fat accumulation and insulin resistance in Japanese men with Type 2 diabetes mellitus, Metabolism 52 (2003) 1274–1278.

[12] B.V. Howard, Lipoprotein metabolism in diabetes mellitus, J. Lipid Res. 28 (1987) 613–628.

[13] M.V. Eynatten, A. Hamann, J.G. Schneider, M. Morcos, P.M. Humpert, J. Kreuzer, et al. Decreased plasma lipoprotein lipase in hypoadipoectinemia. An association independent of systemic inflammation and insulin resistance, Diabetes Care 27 (2004) 2925–2929.

[14] M. Fulop, H.A. Eder, Plasma triglycerides and cholesterol in diabetic ketosis, Arch. Intern. Med. 19 (1989) 1997–2002.

[15] C. Karagianni, S. Stabouli, K. Roumeliotou, J. Traeger-Synodinos, E. Kavazarakis, D. Gourgiotis, et al. Severe hypertriglyceridaemia in diabetic ketoacidosis: clinical and genetic study, Diabetic Med. 21 (2004) 380–382.

[16] P.W. Wilson, E.J. Schaefer, M.G. Larson, J.M. Ordovas, Apoprotein E alleles and risk of coronary disease: a meta-analysis, Arterioscler. Thromb. Vasc. Biol. 16 (1996) 1250–1255.

[17] H. Shimano, S. Ishibashi, T. Murase, T. Gotohda, N. Yamada, F. Takaku, et al. Plasma apolipoproteins in patients with multi-infarct dementia, Atherosclerosis 79 (1989) 257–260.

[18] E.H. Corder, A.M. Saunders, W.J. Strittmatter, D.E. Schmechel, P.C. Gaskell, G.W. Small, et al. Gene dose of apolipoprotein E type 4 allele and the risk of Alzheimer's disease in late onset families, Science 261 (1993) 921–923.

[19] G. Ghiselli, E.J. Schaefer, L.A. Zech, R.E. Gregg, H.B. Brewer Jr., Increased prevalence of apolipoprotein E4 in type V hyperlipoproteinemia, J. Clin. Invest. 70 (1982) 474–477.

[20] F. Fumeron, D. Rigaud, M.C. Bertiere, S. Bardon, C. Dely, M. Apfelbaum, Association of apolipoprotein epsilon 4 allele with hypertriglyceridemia in obesity, Clin Genet. 34 (1988) 258–264.

[21] Y.A. Kesaniemi, C. Ehnholm, T.A. Miettinen, Intestinal cholesterol absorption efficiency in man is related to apoprotein E phenotype, J. Clin. Invest. 80 (1987) 578–581.

[22] J. Kobayashi, Y. Saito, K. Taira, M. Hikita, K. Takahashi, H. Bujo, et al. Effect of apolipoprotein E3/4 phenotype on postprandial triglycerides and retinyl palmitate metabolism in plasma from hyperlipidemic subjects in Japan, Atherosclerosis 154 (2001) 539–546.

[23] M.M. Schreiber, S.I. Shapiro, Secondary eruptive xanthoma, Arch. Derm. 100 (1969) 601–603.

[24] T. Oguni, N. Takeuchi, F. Shigemi, Eruptive xanthoma in a patient with diabetes mellitus, Rinsho Derma (Tokyo) 26 (1984) 251–254 (in Japanese).

[25] K. Tsukamoto, N. Teramoto, R. Saito, K. Maruyama, A case of diabetic xanthoma, Rinsho Derma (Tokyo) 28 (1986) 363–366 (in Japanese).

[26] M. Kawano, Y. Sakamoto, K. Takai, T. Saito, A. Matsuda, T. Kuzuya, et al. An autopsy case of acute necrotizing pancreatitis following hyperlipidemia in a juvenile onset diabetic woman, J. Japan Diab. Soc. 29 (1986) 531–538 (in Japanese, Abstract in English).

[27] N. Suzuki, S. Okabe, I. Itoh, Diabetic xanthoma, Hifubyoshinryo 11 (1989) 51–54 (in Japanese).

[28] K. Yamada, H. Mukai, S. Tomizawa, M. Yokoyama, A case of diabetic xanthoma, Rinsho Derma (Tokyo) 32 (1990) 399–404 (in Japanese).

[29] Y. Hasegawa, M. Yasuhara, H. Nishimura, Diabetic xanthoma with peculiar clinical features, Rinshohifu 47 (1993) 953–958 (in Japanese).

[30] Y. Mizoguchi, Y. Toma, K. Tokuhashi, T. Ochiai, H. Suzuki, T. Morishima, A case of eruptive xanthoma whose eruptions were flattened only by the diet therapy of diabetes mellitus, Rinshohifu 45 (1991) 791–794 (in Japanese).

[31] A. Hashimoto, R. Saitoh, Diabetic xanthoma, Hifubyoshinryo 13 (1991) 41–44 (in Japanese).

[32] T. Nanba, S. Kawakita, Y. Kitajima, Eruptive xanthoma, Rinsho Derma (Tokyo) 38 (1996) 1160–1161 (in Japanese).

[33] T. Kashiwagi, S. Nakamura, H. Iizuka, H. Kubo, Eruptive xanthoma associated with type IV hyperlipoproteinemia, Rinsho Derma (Tokyo) 40 (1998) 197–200 (in Japanese).
[34] S. Honjo, O. Urushibata, T. Hasegawa, R. Saito, Eruptive xanthomatosis in a patient of NIDDM, Rinsho Derma (Tokyo) 42 (2000) 1361–1364 (in Japanese).
[35] Y. Sato, Y. Kawahara, M. Sugawara, Eruptive xanthoma, Hifubyoshinryo 23 (2001) 501–504 (in Japanese).
[36] P.P. Hentges, C.J. Huerter, Eruptive xanthomas and chest pain in the absence of coronary artery disease, Cutis 67 (2001) 299–302.
[37] K. Wakamatsu, I. Miyazawa, T. Gomi, Diabetic xanthoma, Hifubyoshinryo 23 (2001) 353–356 (in Japanese).
[38] K.R. Nayak, R.G. Daly, Eruptive xanthomas associated with hypertriglyceridemia and new-onset diabetes mellitus, N. Engl. J. Med. 350 (2004) 1235.
[39] F. Ramirez, B. Gayraud, L. Pereira, Marfan syndrome: new clues to genotype-phenotype correlations, Ann. Med. 31 (1999) 202–207.
[40] T. Yamamoto, F. Inoue, A. Matsumura, A. Kinugasa, T. Sawada, S. Hayashi, et al. Report of a Japanese girl with Marfan syndrome associated with insulin-dependent diabetes mellitus, Acta Paediatr. Jpn. 34 (1992) 551–553.

nature neuroscience

High cholesterol level is essential for myelin membrane growth

Gesine Saher[1], Britta Brügger[2], Corinna Lappe-Siefke[1], Wiebke Möbius[3], Ryu-ichi Tozawa[4], Michael C Wehr[1], Felix Wieland[2], Shun Ishibashi[5] & Klaus-Armin Nave[1,6]

Cholesterol in the mammalian brain is a risk factor for certain neurodegenerative diseases, raising the question of its normal function. In the mature brain, the highest cholesterol content is found in myelin. We therefore created mice that lack the ability to synthesize cholesterol in myelin-forming oligodendrocytes. Mutant oligodendrocytes survived, but CNS myelination was severely perturbed, and mutant mice showed ataxia and tremor. CNS myelination continued at a reduced rate for many months, and during this period, the cholesterol-deficient oligodendrocytes actively enriched cholesterol and assembled myelin with >70% of the cholesterol content of wild-type myelin. This shows that cholesterol is an indispensable component of myelin membranes and that cholesterol availability in oligodendrocytes is a rate-limiting factor for brain maturation.

During vertebrate brain development, oligodendroglial cells ensheath axonal processes, assemble compact myelin and form the white matter. Myelin provides electrical insulation to the axon and is essential for rapid saltatory impulse conduction. Each myelin sheath represents a spiral extension of the oligodendroglial plasma membrane and appears in cross-sections as a compact, multilayered stack of membranes[1]. In addition to myelin-specific membrane proteins, myelin contains an exceptionally high content of lipids (70% of dry weight). Moreover, more than 25% of the total lipid content is cholesterol, compared to less than 20% in other plasma membranes[2]. Notably, cholesterol is not imported to the brain from the circulation[2].

Based on *in vitro* observations, cholesterol has been implicated in several subcellular functions. It fulfills structural tasks within membranes, such as influencing membrane thickness and fluidity[3], as well as limiting ion leakage through membranes[4], which may be relevant to its property of electrical insulation. Cholesterol, glycosphingolipids and certain membrane proteins can be copurified as detergent-insoluble membrane (DRM) complexes[5]. These complexes have been proposed to correspond to cellular membrane microdomains ('rafts') that serve as platforms for protein sorting[5] and signal transduction[6]. Recently, it has been suggested that myelin membranes may result from the accumulation of myelin-specific rafts in which cholesterol is closely associated with myelin membrane proteins[7,8].

Neither the complete disruption of cholesterol synthesis nor its chemical modulation permits investigation of the role of cholesterol in brain maturation. Previous attempts to study cholesterol function involved chemical extraction[9], a procedure that is not applicable *in vivo*. Chemical inhibitors[10] such as statins modulate cholesterol synthesis but are too nonspecific and toxic when given at concentrations sufficient to shut off cholesterol synthesis[10]. For *in vivo* analysis, we have chosen squalene synthase (SQS; farnesyl-pyrophosphate:farnesyl-pyrophosphate farnesyltransferase, EC 2.5.1.21), which catalyzes the condensation of squalene synthase, the first step specific to sterol biosynthesis[11] (**Fig. 1a**). Complete inactivation of this enzyme, or of 3-hydroxy-3-methylglutaryl coenzyme A (HMG-CoA), the rate-limiting enzyme of this pathway, is lethal during embryonic development[12,13].

Here we describe an essential function of cholesterol in CNS myelination by studying mice with a conditional mutation of the SQS gene (*Fdft1*) in oligodendrocytes. Conditional mutants have severely perturbed myelin synthesis, indicating that oligodendrocytes are the producers of cholesterol in normal brain white matter. However, mutant oligodendrocytes survive by using cholesterol from neighboring wild-type cells of other types. Any myelin made has levels of cholesterol close to normal, thus demonstrating that cholesterol availability is the critical prerequisite and a limiting factor (quantitatively) of myelin membrane growth during brain maturation.

RESULTS

Inactivating SQS function in myelin-forming glial cells

We generated a conditional allele of the *Fdft1* gene in the mouse by introducing two *lox*P sites flanking exon 5 (**Fig. 1b,c**). Exon 5 of *Fdft1* encodes the active site of the enzyme[14]; removal of exons 4 and 5 inactivates SQS function in a conventional *Fdft1* null mutant[13]. Mice with the conditional allele, referred to as SQS-flox mice, developed normally (**Fig. 1d** and data not shown).

[1]Department of Neurogenetics, Max Planck Institute of Experimental Medicine, 37075 Goettingen, Germany. [2]Biochemie-Zentrum, Ruprecht-Karls-Universität Heidelberg, 69120 Heidelberg, Germany. [3]Department of Cell Biology, Universitair Medisch Centrum Utrecht, 3584 CX Utrecht, The Netherlands. [4]Department of Metabolic Diseases, University of Tokyo, Tokyo 113-8655, Japan. [5]Department of Medicine, Jichi Medical School, Tochigi 329-0498, Japan. [6]Hertie Institute of Multiple Sclerosis Research, 37075 Goettingen, Germany. Correspondence should be addressed to K.-A.N. (nave@em.mpg.de).

Published online 27 March 2005; doi:10.1038/nn1426

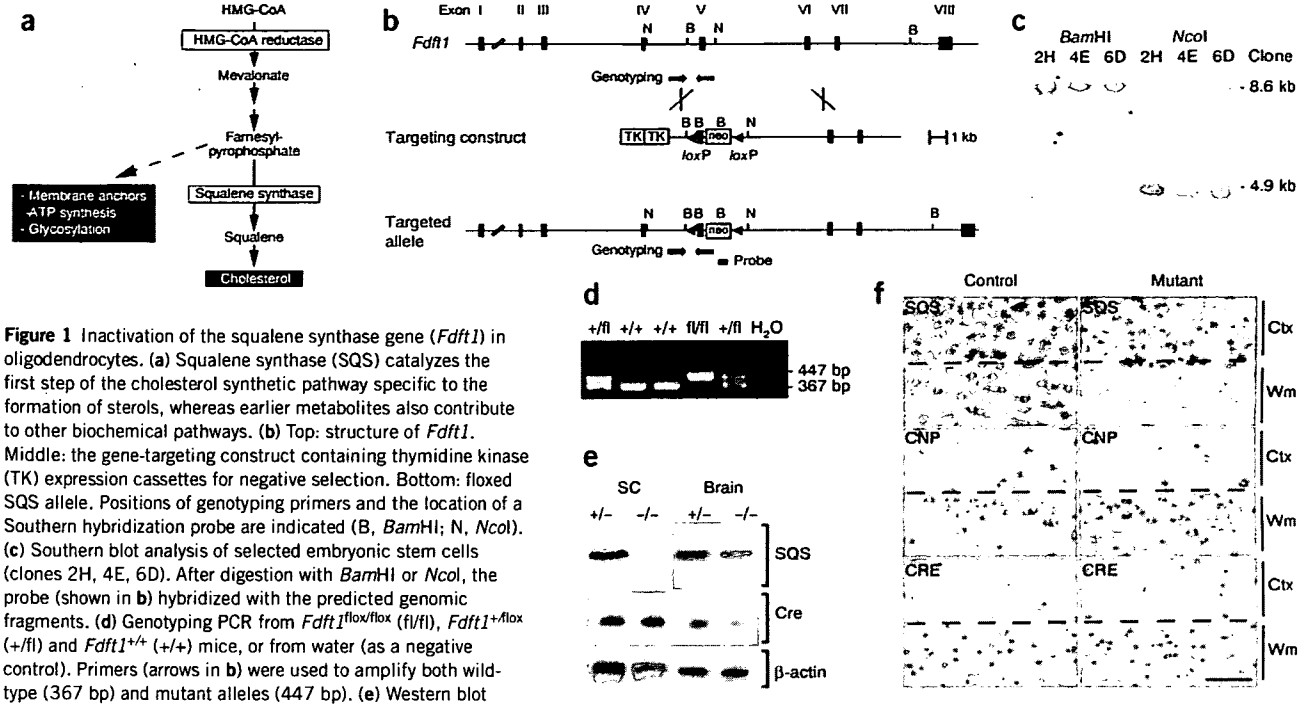

Figure 1 Inactivation of the squalene synthase gene (*Fdft1*) in oligodendrocytes. (**a**) Squalene synthase (SQS) catalyzes the first step of the cholesterol synthetic pathway specific to the formation of sterols, whereas earlier metabolites also contribute to other biochemical pathways. (**b**) Top: structure of *Fdft1*. Middle: the gene-targeting construct containing thymidine kinase (TK) expression cassettes for negative selection. Bottom: floxed SQS allele. Positions of genotyping primers and the location of a Southern hybridization probe are indicated (B, *Bam*HI; N, *Nco*I). (**c**) Southern blot analysis of selected embryonic stem cells (clones 2H, 4E, 6D). After digestion with *Bam*HI or *Nco*I, the probe (shown in **b**) hybridized with the predicted genomic fragments. (**d**) Genotyping PCR from $Fdft1^{flox/flox}$ (fl/fl), $Fdft1^{+/flox}$ (+/fl) and $Fdft1^{+/+}$ (+/+) mice, or from water (as a negative control). Primers (arrows in **b**) were used to amplify both wild-type (367 bp) and mutant alleles (447 bp). (**e**) Western blot analysis of SQS (48 kDa) and Cre (38 kDa) in total brain and spinal cord lysates, prepared from P20 controls (+/−) and mutants (−/−). Comparable staining of β-actin demonstrates equal loading of protein. (**f**) *In situ* hybridization of cortex (Ctx) and subcortical white matter (Wm) of P17 mice using riboprobes (SQS, top; CNP, middle). Arrowheads point to white matter oligodendrocytes of mutant mice that express CNP but did not express SQS. Labeling of oligodendrocytes for Cre (bottom) confirms that targeted cells are not lost. Scale bar, 50 μm.

To inactivate cholesterol biosynthesis in oligodendrocytes, we crossed SQS-flox mice with mice expressing Cre under the control of the 2′,3′-cyclic nucleotide phosphodiesterase (CNP) promoter (referred to as CNP-Cre mice)[15]. In CNP-Cre mice, Cre expression is restricted almost exclusively to oligodendrocytes and Schwann cells and, like expression of CNP (encoded by the gene *Cnp1*), is first detectable in oligodendrocyte precursor cells[15–17]. In subsequent generations, we obtained mice with the genotype $Fdft1^{flox/flox}Cnp1^{+/Cre}$, referred to as 'SQS mutants' or '−/−'. Healthy littermates with the genotype $Fdft1^{+/flox}Cnp1^{+/Cre}$ are referred to as 'controls' or '+/−'. Both mutants and controls were thus heterozygous for *Cnp1*; control mice developed normally[15].

Mutant mice were born at the expected mendelian ratio and were indistinguishable from controls at birth. To verify the genetic defect, we determined the amount of SQS protein by western blotting of brain and spinal cord lysates at postnatal day 20 (p20) and found a quantitative reduction of SQS in mutants (**Fig. 1e**).

To prove inactivation of *Fdft1* in oligodendrocytes, we assessed the expression of SQS mRNA by *in situ* hybridization using a riboprobe specific for exon 5 of SQS mRNA, to distinguish Cre-recombinant from wild-type cells. In control mice, we detected SQS mRNA in almost all brain regions (**Fig. 1f**, upper left). In contrast, mutant animals largely lacked SQS-specific signals in the white matter, such as the corpus callosum (**Fig. 1f**, upper right). The SQS-deficient cells were oligodendrocytes, as judged by their size and characteristic arrangement in chains. Moreover, *in situ* hybridization of CNP mRNA labeled the same group of cells (**Fig. 1f**, middle) that lacked SQS mRNA. When oligodendrocytes from neonatal mutant mice were maintained in cell culture and immunostained, virtually all CNP-positive cells also were Cre-positive and showed strongly diminished SQS signals (**Supplementary Fig. 1** online). Thus, all oligodendrocytes showed evidence of Cre-mediated recombination leading to the subsequent loss of SQS expression.

We determined the density of Cre-positive cells in white matter in tissue sections from P20–P100 mice, which showed that mutant oligodendrocytes were present and did not reveal any obvious cell loss (**Fig. 1f**). In the corpus callosum at P20, we counted $3.4 \times 10^3 \pm 0.5 \times 10^3$ cells/mm^2 in mutants, compared to $3.0 \times 10^3 \pm 0.3 \times 10^3$ cells/mm^2 in controls on comparable 4-μm sections. Moreover, western blotting of brain extracts showed an equal steady-state abundance of Cre protein (**Fig. 1e**). With TUNEL staining, we found the same low number of apoptotic cells in the brain (fewer than five cells per coronal section; data not shown), providing independent evidence that oligodendrocyte death was not unusually prevalent.

Ataxia, tremors, and premature death

Despite their identical appearance at birth, mutant mice lagged behind controls in weight gain, and although both sexes were fertile, mutants' overall breeding performance was poor. All mutant mice developed motor function deficits at about 2 weeks of age, coinciding with the known peak of CNS myelination in wild-type mice. The deficits included ataxia, initiation tremor and impaired control of hindlimb movements (**Fig. 2a** and **Supplementary Video 1** online). When quantified by rotarod testing at P20, the motor performance of all mutants was markedly lower than that of controls (**Fig. 2b**).

About one-third of mutant mice died between 20 and 30 d (**Fig. 2c**). Notably, mutants that survived past 1 month of age rarely died prematurely, suggesting that older animals had overcome a critical period in this disorder. The probability of premature death was

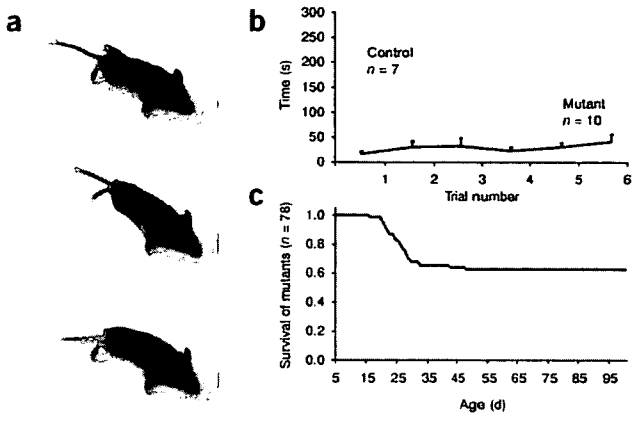

Figure 2 Clinical phenotype. (**a**) Consecutive frames (25 Hz) taken from a video clip of 20-d-old mutant mice, with tremor and ataxia (**Supplementary Video 1**). (**b**) Analysis of motor performance of P20 mice using a standardized accelerating rotarod test with six trials. Mutant mice (black) showed worse motor performance than littermate controls (gray) when total holding time was scored. Values are expressed as mean ± s.e.m. (**c**) Kaplan-Meier survival curve of mutant animals ($n = 78$). About one-third of mutant mice died during the third and fourth weeks; after that point, the clinical phenotype seemed to be stable.

unrelated to the severity of the motor function defect. Premature death may be caused by lethal seizures, although we never observed acute seizures.

Hypomyelination of CNS white matter

On histological sections, we visualized myelin by Gallyas silver impregnation[18] and immunostained for the myelin-specific proteins proteolipid protein (PLP/DM20, encoded by *Plp1*) and CNP. There was a severe dysmyelination of the spinal cord white matter, which was almost devoid of myelin at P20 (**Fig. 3a**). The corpus callosum (**Fig. 3a**) and the cerebellar white matter (data not shown) also showed a marked reduction of myelin staining in mutant mice. We confirmed the severe dysmyelination of white matter fiber tracts by electron microscopy of lumbar spinal cord (**Fig. 3b**). In mutant mice, most axons showed abnormally thin myelin sheaths or were unmyelinated. In contrast, in gray matter areas such as the central spinal cord, myelin appeared nearly normal and axons showed little difference in myelin thickness (**Fig. 3b**).

To estimate the degree of hypomyelination semiquantitatively, we determined the ratio of myelinated axons in the lateral funiculus of the thoracic spinal cord ($n = 2$ each) at early stages (P9) and during the peak of myelination (P20). In control mice, 58 ± 7% of axons possessed a thin myelin sheath at P9. At P20, virtually all axons (90 ± 2%) were myelinated, and myelin thickness had reached almost adult levels. In contrast, in SQS mutant mice, only a few axons (12 ± 4%) were myelinated at P9, and this fraction increased to only 33 ± 3% at P20. In addition, the myelin thickness in mutant mice never reached control levels (also see below). Thus, myelination was affected early in the assembly process.

Taken together, these results indicate that mutant oligodendrocytes are capable of forming myelinating processes but that myelination is quantitatively impaired. The severity of hypomyelination differs markedly between CNS regions. Although we cannot exclude lineage-related differences between oligodendrocytes of white and gray matter, it is more likely that the ability of oligodendrocytes to make myelin is heavily influenced by neighboring wild-type cells.

The *Cnp1* gene is also expressed in myelin-forming Schwann cells. As expected, SQS mutant mice showed dysmyelination of the peripheral nervous system (data not shown), which is likely to contribute to the described motor defects. However, the clinical phenotype described here is clearly dominated by spinal dysmyelination. A detailed account of the peripheral neuropathy will be reported elsewhere.

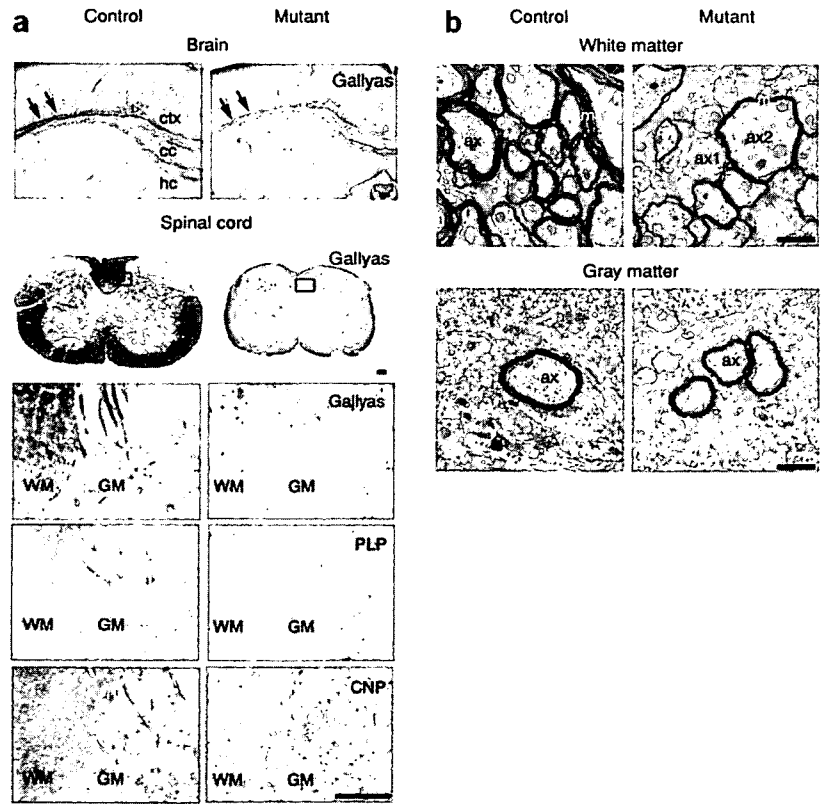

Figure 3 Hypomyelination of CNS white matter tracts. (**a**) Sections of brain and spinal cord of P20 animals were impregnated with silver to visualize myelin (Gallyas) or were immunostained for myelin proteins (PLP and CNP). Arrows point to the corpus callosum (cc), which is hypomyelinated in the mutant brain (ctx, cortex; hc, hippocampus). Dysmyelination of white matter tracts is more obvious in the spinal cord. Boxed areas indicate the position of detailed views shown below (GM, gray matter; WM, white matter; scale bar, 100 μm). (**b**) Ultrastructural analysis of spinal cord at P20. In white matter of control animals (left), virtually all axons (ax) are myelinated, whereas fibers in mutants (right) possess a thin myelin sheath or lack myelin. This dysmyelinating phenotype is less pronounced in gray matter, where axons have myelin of comparable thickness in both control and mutant mice (ax1, unmyelinated axon; ax2, axon with thinner myelin; m, myelin; scale bar, 1 μm).